



URock 2023a: An open source GIS-based wind model for complex urban settings

Jérémy Bernard^{1,2,3}, Fredrik Lindberg¹, and Sandro Oswald⁴

¹University of Gothenburg, Department of Earth Sciences, Sweden

²University of Savoie Mont-Blanc, LOCIE, UMR 5271, France

³CNRS, Lab-STICC, UMR 6285, Vannes, France

⁴Institute of Meteorology, University of Natural Resources and Life Science (BOKU), Vienna, Austria

Correspondence: Jérémy Bernard (jeremy.bernard@zaclys.net)

Abstract. URock 2023a is an open source diagnostic model dedicated to wind field calculation in urban setting. It is based on a quick method initially proposed by Röckle and already implemented in the proprietary software QUIC-URB. First, the model method is described as well as its implementation in the free and open source geographic information system called QGIS. Then it is evaluated against wind tunnel measurements and QUIC-URB simulations for four different building settings plus one case with an isolated tree. The correlation between URock and QUIC-URB is high and URock reproduces quite well the spatial variations of the wind speed observed in the wind tunnel experiments. Sources of improvements are highlighted, which are applicable both for URock and QUIC-URB. URock 2023a is available via the Urban Multiscale Environment Predictor (UMEP), a city-based climate service tool designed for researchers and service providers presented as a plugin for QGIS. The model, data and scripts used to write this manuscript can be freely accessed at <https://zenodo.org/record/7681245>.

10 1 Introduction

Due to climate change, thermal comfort is getting an important topic in the urban planning process. An outdoor space should be comfortable during summer time but also remains comfortable during winter time. Shortwave and longwave radiation, wind speed, air temperature and relative humidity are the main meteorological variables that impact the human heat balance. Radiation and wind speed are the variables the most spatially sensitive to a small variation of an urban configuration: a new building will create shadow and also in most cases decrease the wind downstream. This will affect the outdoor thermal comfort and the weather conditions at the buildings boundaries which may also impact indoor thermal comfort. Thus, there is a need for easy to use tools to calculate the level of radiation received by surfaces in an urban setting and also the spatial variations of the wind. Several tools already exist to achieve this work such as Envi-met (Huttner and Bruse, 2009; Bruse, 2004), SkyHelios (Matzarakis et al., 2021), Solene-microclimate (Morille et al., 2015; Musy et al., 2021) or (Kastner and Dogan, 2022). However, these tools are proprietary softwares (or not publicly available concerning Solene-microclimate) making their use difficult for community development purpose. PALM is a 3D, CDF modelling system that can be used to predict the wind in urban area using the PALM-4U components (Maronga et al., 2020). It is designed to model complex physical phenomenons and is thus not dedicated to run large areas on a personal computer. More recently, an open source model (QES-Winds) based on the



QUIC-URB one has been developed by Bozorgmehr et al. (2021). Urban Multi-scale Environmental Predictor (UMEP) is a
25 climate service tool that can be used for a wide variety of applications including thermal comfort (Lindberg et al., 2018). It is
developed as a plugin available in the free and open source QGIS software. This integration facilitates the user interaction
with spatial information to determine model parameters, and to edit, map and visualise inputs and results. For this reason,
this cross-platform, free and open source tool is well suited for both researcher and practitioners within the field or urban
climatology. However, it does not have any model dedicated to wind calculation yet. This article presents the URock model,
30 which has been recently developed and added into UMEP.

The requirement specifications were to have a relatively fast and accurate model, simple of use and resulting in a wind
field that can be used for indoor and outdoor applications (comfort and pollution). Many options were considered: prognostic
models, statistical models and diagnostic models. The first consists in solving the Navier-Stokes equations through numerical
methods. While this is probably the most accurate method, it is also the slowest and needs a certain degree of expertise for a user
35 to have relevant results (Tominaga et al., 2008). The second consists in using relationships that have been established between
observed or simulated wind speed fields and a given set of explanatory variables such as distance to a wall or a tree, sky view
factor, etc. (Calzolari and Liu, 2021; Johansson et al., 2016). However, these relations are only valid for cases where the urban
setting remains quite close from the one(s) used to create the model. It can then be quite inaccurate in some specific urban
settings (Johansson et al., 2016). Moreover, atmospheric pollution and building applications need a three dimensional field and
40 for the three components of the wind, rendering the statistical modelling quite inappropriate. The last option, called diagnostic
model, is a good compromise between the two first. It is a two steps approach: in the first step, the wind speed and wind
direction are initialized in several zones around wind obstacles. The location and size of the zones as well as the values used
for wind speed and wind direction are derived from wind tunnel observations. The second step consists in balancing the air flow
while minimizing the modifications of the initial wind field. Initially, this method was implemented at larger scale (buildings
45 were not considered) to take into account the effect of terrain elevation on the wind (Sherman, 1978; Ratto et al., 1994). At this
scale, the initialization stage is not based on empirical laws deduced from wind tunnel experiments but performed using wind
observations: the wind speed is initialized in locations where wind observations are available. The resulting wind field using
this method is in quite good agreement with observations or wind fields derived from prognostic models (Wellens et al., 1970).
Röckle (1990) was the first to propose a quite detailed set of empirical laws to initialize the wind speed around buildings. At
50 our knowledge, the first software implementation of its work, called QUIC-URB, has been developed by Pardyjak and Brown
(2003) and is available on request as a proprietary software. Several modifications have been performed to improve the model
accuracy: some of the empirical laws proposed by Röckle (1990) have been modified and new zones have also been created
(Bagal et al., 2004; Pol et al., 2006; Nelson et al., 2009). The QUIC software is initially dedicated to pollution dispersion but
the 3D wind field generated by QUIC-URB can also be used for outdoor thermal comfort applications (Girard et al., 2018) and
55 for building energy or building thermal comfort applications thanks to a pressure solver model (Brown et al., 2009b). Recently,
Fröhlich (2016) and Fröhlich and Matzarakis (2018) have implemented in SkyHelios a diagnostic model which is also based
on the Röckle (1990) methodology and the QUIC-URB improvements. However, as previously highlighted, these models are
not available as free and open source code. Moreover, the methodology used for the initialization step is not fully described.



This article presents the detailed methodology used by the free and open source diagnostic model URock which has been
60 implemented in UMEP (Sect. 2). Its implementation in UMEP is described Sect. 3. Several wind tunnel experiment data are
freely available thanks to the Architectural Institute of Japan (AIJ). These data are used to verify that URock reproduces well
the wind field generated by QUIC-URB and also to investigate what are the main modifications that could be performed in
these current diagnostic models to improve their accuracy (Sect. 4).

2 Model description

65 URock can be used to calculate the 3D wind field of an urban area using information about the wind (at least speed and
direction at a given height) and geographical data describing the area of interest (building and vegetation footprint and height).
Two main stages are used: wind field initialization and wind field balance.

The wind field is initialized according to empirical laws drawn from wind tunnel experiments. As QUIC-URB is nowadays
the most validated diagnostic model, all zones and their corresponding empirical laws used in URock are the ones also used in
70 QUIC-URB. In URock, nine different zones are identified around buildings and within vegetation:

- Six belong to isolated buildings (Fig. 1a),
- A single zone (the so-called street-canyon) is created between two buildings close to each other (Fig. 1b).
- Two distinct zones are created within vegetation depending of their proximity with buildings (Fig. 1c).

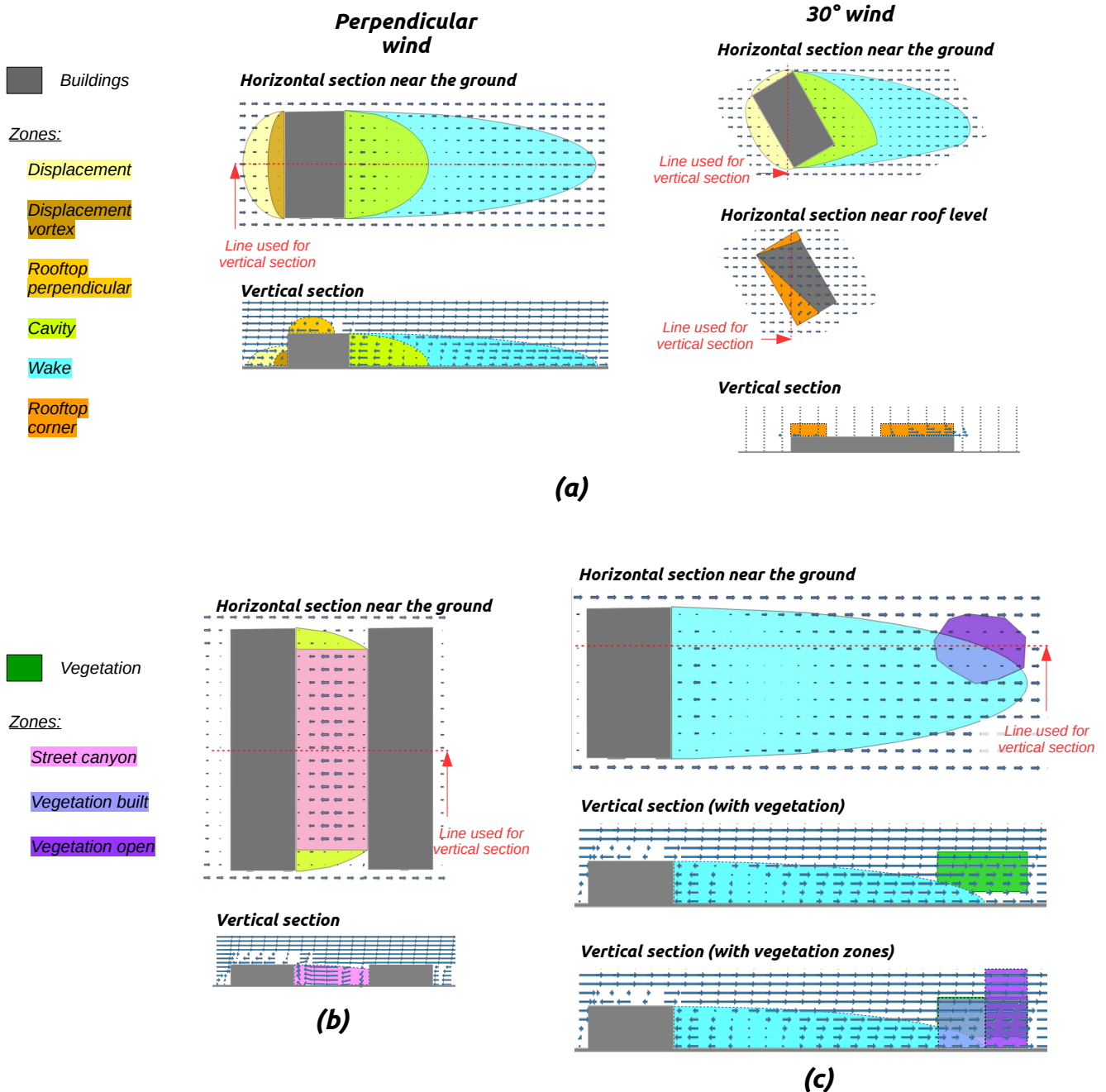


Figure 1. Illustration of the nine zones used in URock to initialize the wind field: (a) zones created by isolated building, (b) zones created between nearby buildings and (c) zones created within vegetation.

The size of each of these zones is calculated from obstacle properties (such as height, length and width for building or
 75 attenuation capacity for the vegetation). The wind speed and wind direction depends on the zone type and location within the



zone (distance to the wall, to the ground or the end of the zone). More informations about each of the zones will be given Sect. 2.3.2 (building zone size), 2.3.3 (vegetation zone size) and 2.3.4 (building and vegetation wind factors).

The wind field is then numerically balanced in order to make it physically relevant with the constraint to minimize the differences with the initial wind field.

80 The algorithm used in URock is based on the following procedure (illustrated Fig. 2):

1. Create URock geometries: the input geographical data is initialized into the format needed for the URock calculations,
2. Effect of all obstacles on the wind: some morphometric properties of the study area are calculated and can be used to set a mean wind profile,
3. Effect of individual obstacles on the wind: each obstacle is considered individually to set the initial wind factor near buildings and within vegetation,
- 85 4. Calculates wind speed: the 3D wind speed components are initialized for each cell of the sketch and then used in the numerical solver to get the final balanced wind field.

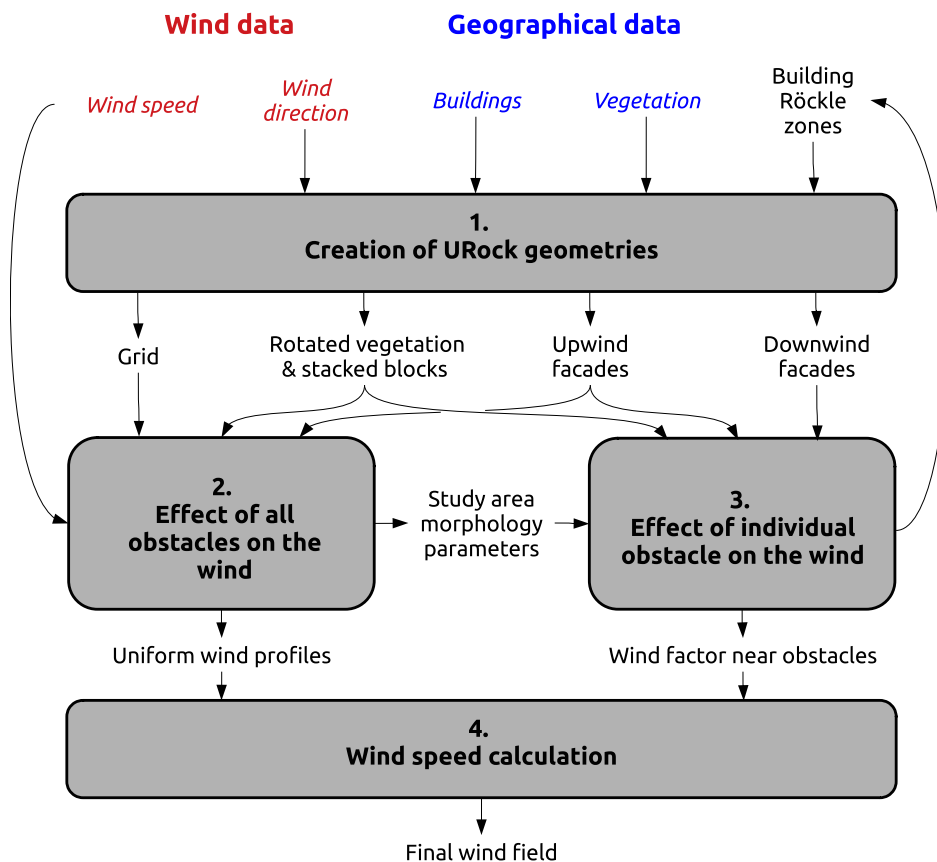


Figure 2. Overall methodology used by the URock model



Each step of this procedure will be described in the following subsections.

2.1 Creation of URock geometries

90 This step is dedicated to the transformation of standard input vector geometries into a format that will facilitates the wind speed initialization and also to create the grid used for numerical solving. The following processes are used (Fig. 3). First, individual buildings are converted to stacked blocks. Then, the entire sketch (buildings and vegetation) is rotated to always have the wind coming from North. Last, a 3D grid of rectangular-based cells is created and the facades being upwind as well as those being downwind are identified.

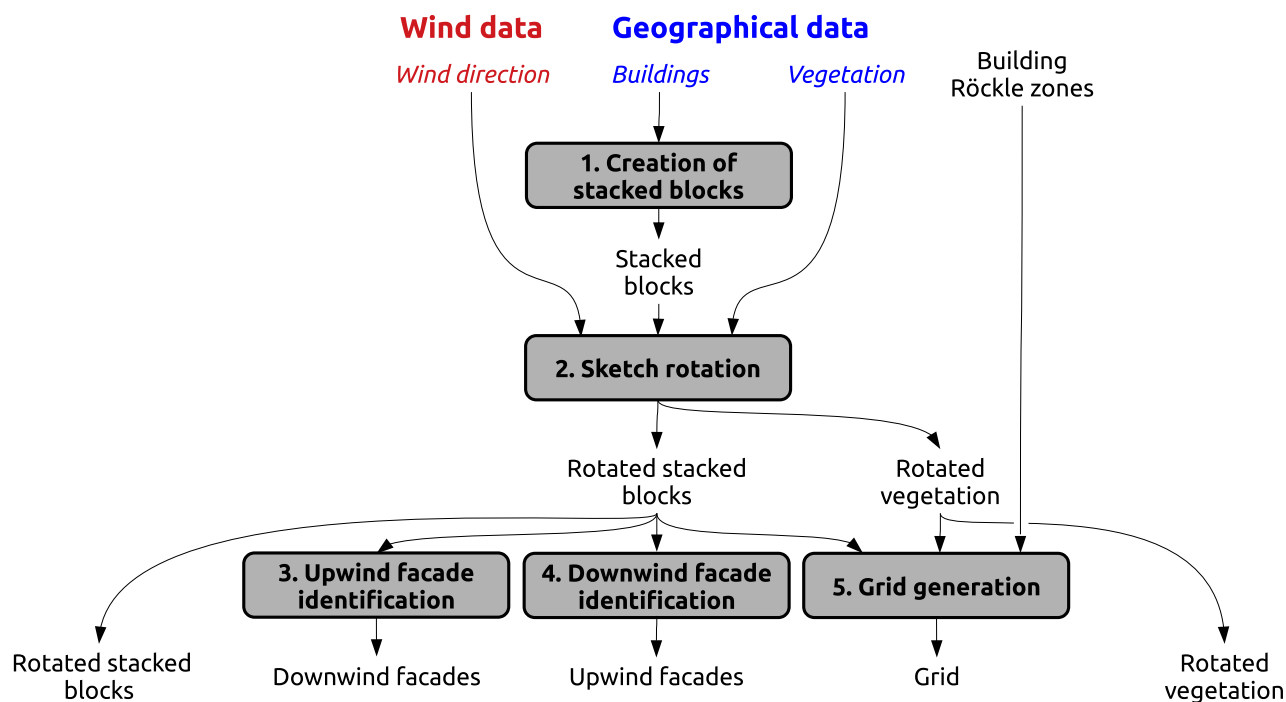


Figure 3. Procedure used to create the URock geometries

95 2.1.1 Creation of stacked blocks

Buildings may have an oversampled number of points, which may result in a considerable amount of Röckle zones (some of the zones are created for each unique segments) and thus results in low computation efficiency. To avoid such issue, building geometries are first simplified removing useless points¹.

The size of a Röckle zone depends on the size of the obstacle. In URock, buildings touching each other but having a different height are transformed into vertically stacked blocks as shown in Fig. 4 (method also used in QUIC-URB). A preliminary task

¹This is done using the H2GIS ST_Simplify function (http://www.h2gis.org/docs/dev/ST_Simplify/) with distance = GEOMETRY_SIMPLIFICATION_DISTANCE (default 0.25 m)



is to merge buildings touching each other or being within a given distance to each other. A buffer is created around each building² and the footprints touching each other are spatially unioned. Then, we round building height values and we create as many stacked blocks as there are isolated blocks of same height.

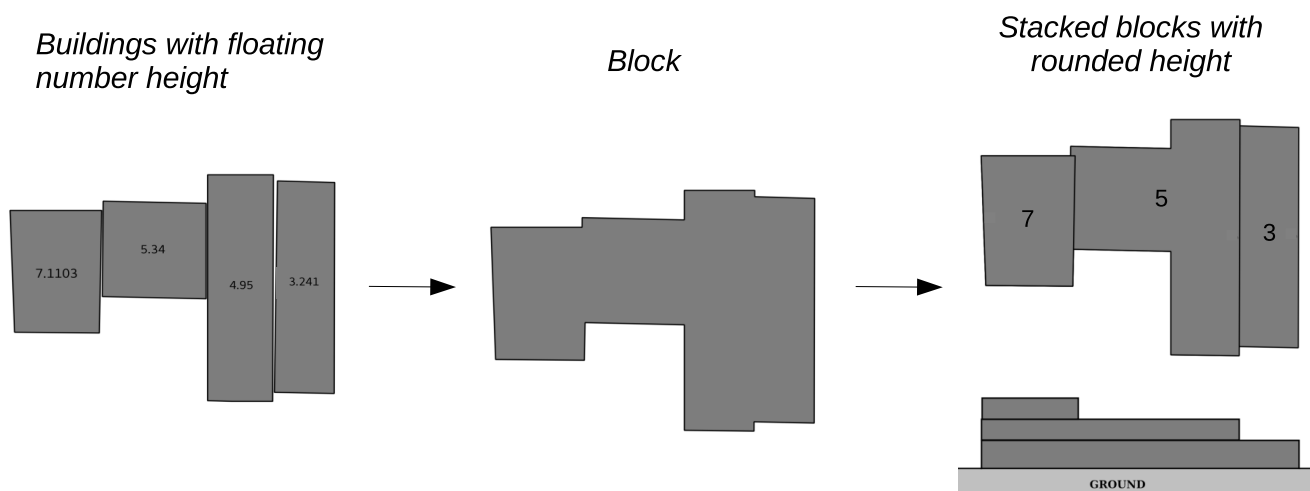


Figure 4. Method used to convert buildings to stacked blocks

2.1.2 Sketch rotation

105 All obstacles are rotated in order to have the wind coming downward to simplify the equations used in the initialization step. The rotation center is defined as the top right corner of the smallest bounding box containing all obstacles.

2.1.3 Upwind facades identification

Each facade (defined as individual segment belonging to a given stacked block) facing the wind is identified in order to apply the displacement zone scheme. This scheme affects from the bottom of the facade and up to 60% of the facade height. Thus
 110 first several facades belonging to (or nearby) a same vertical plan are merged in order to avoid unexpected displacement zone scheme such as illustrated Fig. 5a³. The facade base height $H_{FB_{i+1}}$ (H_{FB_1} in Fig. 5b) of the upper stacked block is then set to the base height of the bottom stacked block.

²This is done using the H2GIS ST_BUFFER function (http://www.h2gis.org/docs/dev/ST_Buffer/) with bufferSize = SNAPPING_TOLERANCE (default 0.3 m) and bufferStyle='join=mitre'

³a facade from an upper stacked block is snapped to the facade of the lowest stacked block if sufficiently close using the function ST_SNAP (http://www.h2gis.org/docs/dev/ST_Snap/) with a snapTolerance = SNAPPING_TOLERANCE (default 0.25 m)

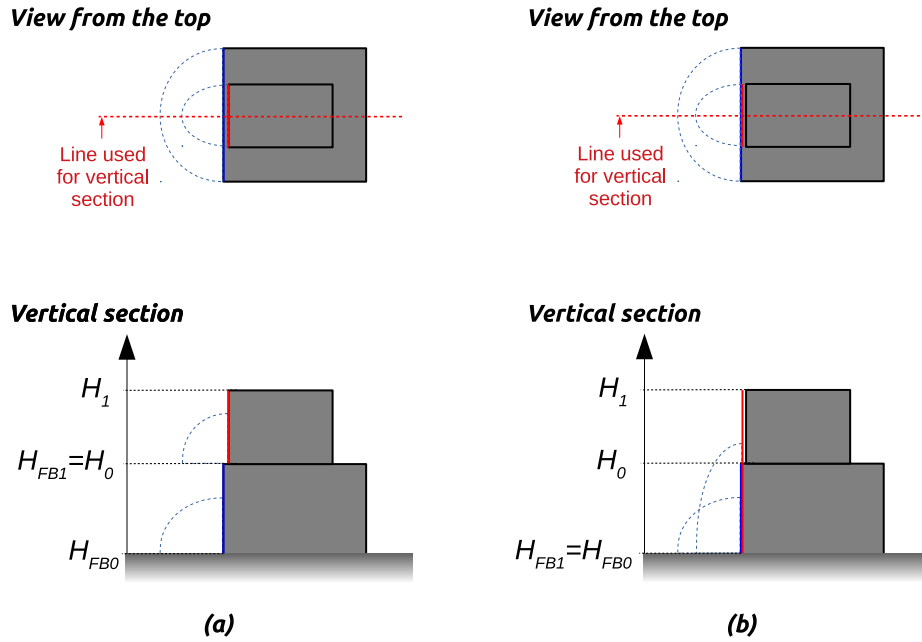


Figure 5. Facade base height and displacement zone of an upper stacked block if the facade is (a) outside or (b) within the snapping tolerance

2.1.4 Downwind facades identification

Each downwind facade (defined as linestring - multisegments connected to each other) is identified in order to apply the cavity and wake zone schemes. Wake zones are defined from the ground while cavity zones starts at cavity base height (H_{CB}). In URock, the cavity zone of a stacked block i may alter the cavity zone of the stacked block $i-1$ located below up to its cavity base height (H_{CB_i} - Fig. 6). This property is defined Eq. 1 ((Brown et al., 2009a)).

$$H_{CB_i} = H_{B_i} - \frac{L_i}{L_{i-1}} \cdot (H_{i-1} - H_{B_{i-1}}) \quad (1)$$

where H_{B_i} is the base height of stacked block i above ground level, $H_{B_{i-1}}$ is the base height of stacked block $i-1$ above ground level, H_{i-1} is the top height of stacked block $i-1$ above ground level, L_i the cross wind width of stacked block i , L_{i-1} the cross wind width of stacked block $i-1$.

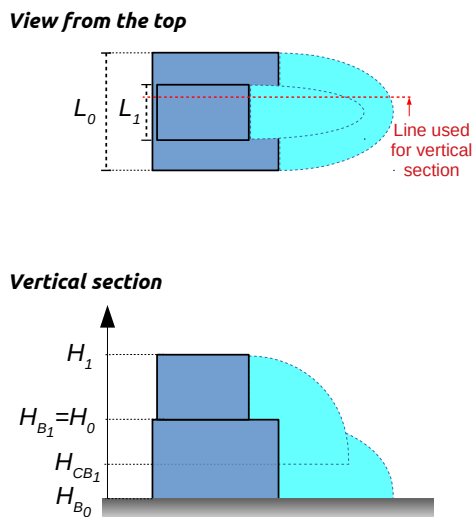


Figure 6. Cavity base zone extension for downwind facades of an upper stacked block

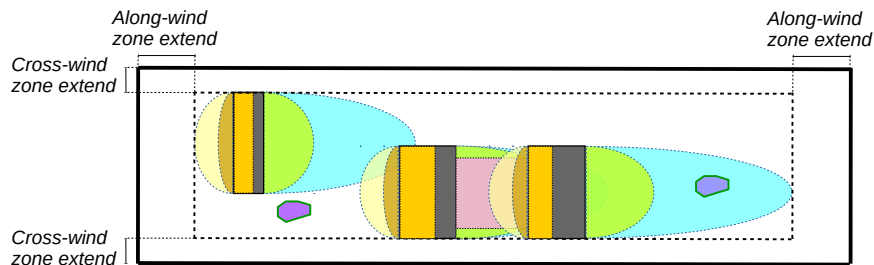
2.1.5 Grid generation

The grid of rectangular-based cells is created according to a horizontal and a vertical resolution set by the user. The size of the grid is defined as an extend distance beyond built Röckle zones and vegetation boundaries (Fig. 7). By default, the values for the extends are 60 m, 40 m and 20 m respectively for along-wind, cross-wind and vertical axis⁴.

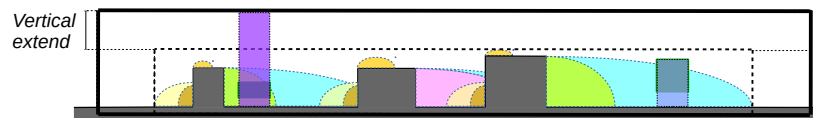
⁴these values can be modified in the code by the user using respectively `ALONG_WIND_ZONE_EXTEND`, `CROSS_WIND_ZONE_EXTEND` and `VERTICAL_EXTEND` variables



View from the top



Vertical section



Geographical data

- Block
- Vegetation

Röckle zones

- Displacement
- Displacement vortex
- Cavity
- Wake
- Street canyon
- Rooftop perpendicular
- Vegetation open
- Vegetation built

Study area boundaries

- Smallest box containing all built Röckle zones and vegetation
- Box used for the numerical solving problem

Figure 7. Domain size definition according to along-wind zone extend, cross-wind zone extend and vertical extend

2.2 Effect of all obstacles on the wind

The vertical wind profile is initialized considering mean roughness properties of the study area (Fig. 8).

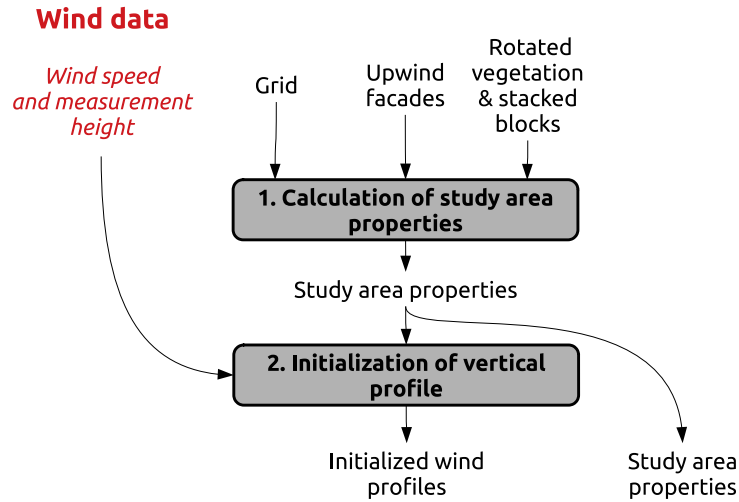


Figure 8. Procedure used takes into account the effect of all obstacles on the wind field

2.2.1 Calculation of study area properties

The roughness height (z_0) and displacement length (d) are both calculated as a unique value characterizing the entire study area. The method described by Hanna and Britter (2002) is used. First the normalized frontal area (λ_f) is calculated as the ratio between the projected frontal area of obstacle facing the wind (A_f) and the area of the smallest rectangle containing all buildings and vegetation (A_T). Then z_0 and d are calculating based on the area-weighted geometric mean obstacle height (H_r) and the (λ_f) value. Note that the equations differ upon (λ_f) values (Tab. 1).

Table 1. Displacement length and roughness height equations depending on the normalized frontal area value. *Note that Hanna et Britter specified that these relations are valid for an upper Hr limit of about 20 m, thus it may lead to higher error if applied to neighborhoods such as skyscrapers.*

Condition	Displacement length d (m)	Roughness height z_0 (m)
$\lambda_f \leq 0.05$	$d = 3 \cdot \lambda_f \cdot H_r$	$z_0 = \lambda_f \cdot H_r$
$0.05 < \lambda_f < 0.15$	$d = 0.15 + 5.5 \cdot (\lambda_f - 0.05)$	$z_0 = \lambda_f \cdot H_r$
$0.15 \leq \lambda_f < 1$	$d = 0.7 + 0.35 \cdot (\lambda_f - 0.15)$	$z_0 = 0.15 \cdot H_r$
$1 \leq \lambda_f$	$d = 1$	$z_0 = 0.15 \cdot H_r$

2.2.2 Initialization of vertical profile

In this URock version, the vertical wind speed profile is set homogeneously on the entire calculation domain. Three possible choices are currently available to set the vertical profile using:

- a power-law such as defined by Pardyjak and Brown (2003) (Eq. 2),



- an urban profile defined as an exponential increase within the canopy (Cionco, 1972) and logarithmic increase above the canopy (Eq. 3),

140 – a user defined profile.

$$V(z) = V_{ref} \cdot \left(\frac{z}{z_{ref}}\right)^p \quad (2)$$

where $V(z)$ is the wind speed at height z above ground level, V_{ref} is the reference wind speed observed (or modeled) at the reference height, z_{ref} is the height above ground level of the reference wind speed, $p = 0.12 \cdot z_0 + 0.18$ is the exponent of the power-law where z_0 is the roughness height of the study area (Matzarakis and Endler, 2009).

$$145 \quad V(z) = \begin{cases} V_{ref} \cdot \exp\left(a \cdot \left(\frac{z}{H_r} - 1\right)\right) & \text{if } z < H_r \\ V_{ref} \cdot \frac{\log\left(\frac{z-d}{z_0}\right)}{\log\left(\frac{z_{ref}-d}{z_0}\right)} & \text{otherwise} \end{cases} \quad (3)$$

where $a = 9.6 \cdot \lambda_f$ is the attenuation coefficient (Macdonald, 2000), λ_f is the normalized frontal area, H_r is the area-weighted geometric mean height of all obstacles, z_0 is the roughness height, d is the displacement length (Tab. 1).

The two first solutions only need a reference height and the corresponding wind speed as input while the second solution needs to have wind speed observed / modeled at several height in the atmosphere.

150 2.3 Effect of individual obstacles on the wind

Obstacles locally alter the wind field: wind direction or/and wind speed may be modified within vegetation and around buildings. The Röckle approach is applied to set an initial wind factor to those locations using seven building schemes and two vegetation ones (Fig. 9). First, stacked block properties are calculated. Then building and vegetation Röckle zones boundaries are identified and the wind factor corresponding to each zone is calculated. Last, some rules are set to keep only one wind

155 factor value when two (or more) Röckle zones overlay.

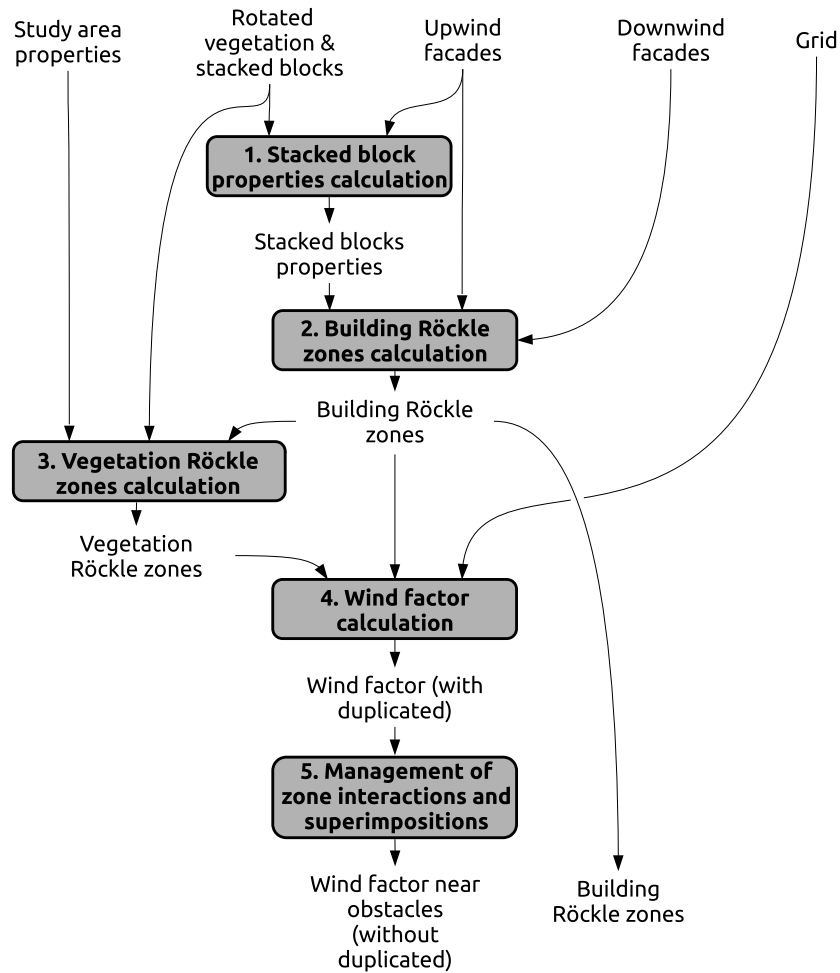


Figure 9. Procedure used to take into account the effect of each individual obstacle on the wind field

2.3.1 Stacked block properties calculation

The stacked block height, effective width (cross-wind width - W_{eff}) and effective length (along wind length - L_{eff}) are the three input parameters used to calculate the building zones. While the definition of the first one have not changed over QUIC-URB versions (difference of height between the top and the base of a stacked block), the definition of the two others have been updated by Nelson et al. (2008) to improve the accuracy of the estimated wind field when the wind was not coming perpendicular to the facade of a rectangular building (Fig. 10).

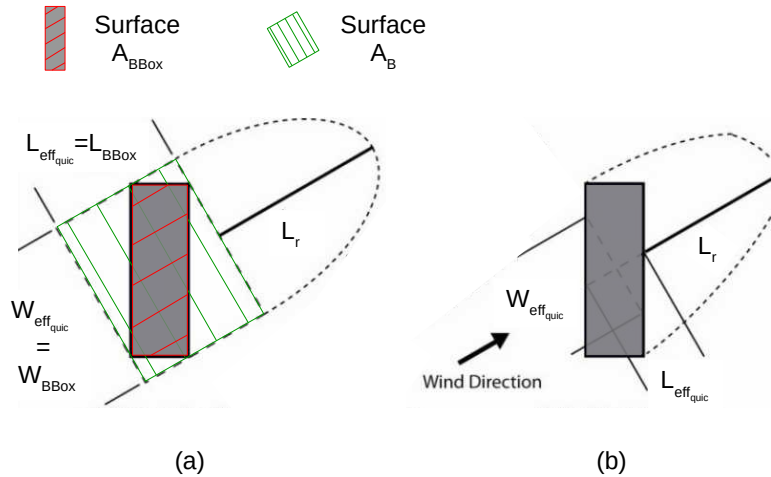


Figure 10. QUIC-URB method to calculate the building effective width and building effective length (a) before and (b) after modifications proposed by Nelson et al. (2008). Source: Adapted from Nelson et al. (2008)

However, their modified algorithm only works for rectangular shape whereas our stacked blocks may have any shape. Thus the effective width and length are calculated using respectively Eq. 4 and 5.

$$W_{eff} = W_{BBox} \cdot \frac{A_B}{A_{BBox}} \quad (4)$$

$$165 \quad L_{eff} = L_{BBox} \cdot \frac{A_B}{A_{BBox}} \quad (5)$$

where W_{eff} is the effective width of the stacked block in URock, L_{eff} is the effective length of the stacked block in URock, W_{BBox} is the cross-wind width of the stacked block bounding box (corresponding to $W_{eff_{quiv}}$ in Fig. 10a), L_{BBox} is the cross-wind length of the stacked block bounding box (corresponding to $L_{eff_{quiv}}$ in Fig. 10a), A_B is the stacked block footprint area (cf Fig. 10a), A_{BBox} is the area of the stacked block bounding box (cf Fig. 10a).

170 2.3.2 Building Röckle zones calculation

This section contains a partial description of the building Röckle zones calculated in URock. More details can be found in the appendix A.

Displacement zone

The displacement zone is defined as a quarter of ellipse located on each upwind facade (cf Fig. 1a) such as defined by Kaplan
 175 and Dinar (1996).

Displacement vortex zone



The displacement vortex zone is defined as a quarter of ellipse located on each upwind facade whenever the angle between the wind direction and an upwind facade $\theta_{wind/upwind_F}$ is within [90-PERPENDICULAR_THRESHOLD_ANGLE, 90+PERPENDICULAR_THRESHOLD_ANGLE] (cf Fig. 1a). The default value for
180 fault value for PERPENDICULAR_THRESHOLD_ANGLE is set to 15° compared to 20° in QUIC-URB (Bagal et al., 2004). The reason for this difference is that the rooftop perpendicular scheme is also activated when the upwind facade is nearby the perpendicular from the wind direction but the condition for activation of the rooftop perpendicular and displacement vortex differs in QUIC-URB (15° for the rooftop perpendicular while 20° for the displacement vortex) while we chose to have consistency between
185 these two schemes in URock. However, the size of the zone is identical in URock and QUIC-URB (Bagal et al., 2004).

Cavity zone

The cavity zone can be seen as a quarter of ellipse but having a slightly modified equation. If a standard ellipse has a fixed center, the one used in URock has a center which moves upon the along-wind direction, following the facade coordinates (cf. Fig. 1a). For complex stacked blocks having multiple downwind facades, this definition results in the cavity zones illustrated
190 Fig. 11. For any downwind facade, the ellipse has the same size at a given coordinate along the cross-wind axis (left to right on the Figure). This is most probably not the case in the reality and thus must be further investigated in future URock versions.

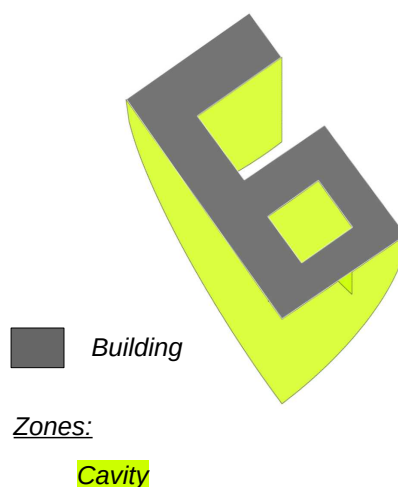


Figure 11. View from the top of the cavity zones created for a complex stacked block

Wake zone

The wake zone comes along with the cavity zone. Thus it has exactly the same shape but is three times longer along-wind (Kaplan and Dinar, 1996).

195 **Rooftop perpendicular zone**



The rooftop perpendicular zone is defined as a half ellipse base cylinder cut along its height and located on each rooftop with lengths consistent with the ones defined by Pol et al. (2006). It is only created when the angle between the wind direction and an upwind facade $\theta_{wind/upwind_F}$ is within [90-PERPENDICULAR_THRESHOLD_ANGLE, 90+PERPENDICULAR_THRESHOLD_ANGLE] (cf Fig. 1a). The default value for PERPENDICULAR_THRESHOLD_ANGLE is set to 15°, the same value as in QUIC-URB (Pol et al., 2006). Note that the rooftop perpendicular zones are only defined above buildings and extend along-wind from upwind facades, leading to cylinders having non parallel bottom and top sections whenever the wind is not perpendicular to the upwind facade.

Rooftop corner zone

The rooftop corner zone is defined as a square base oblique pyramid located on rooftop along an upwind facade with the apex starting from the most upwind point (cf Fig. 1a). The size of the zone is calculated using Bagal et al. (2004) equations. The scheme is activated only when the angle between the wind direction and an upwind facade $\theta_{wind/upwind_F}$ is within +[90+CORNER_THRESHOLD_ANGLE_MIN, 90+CORNER_THRESHOLD_ANGLE_MAX] and the default values for CORNER_THRESHOLD_ANGLE_MIN and CORNER_THRESHOLD_ANGLE_MAX are respectively 30 and 70°.

Street canyon zone

The street canyon zone is created between two stacked blocks when the upstream building cavity zone intersects an upwind facade of a downstream building.

2.3.3 Vegetation Röckle zones calculation

Similarly as QUIC-URB (Nelson et al., 2009), two different schemes are dedicated to the vegetation in URock: one when the vegetation is located within a building influence (vegetation in built-up area) and the other when is is far from building influence (vegetation in open area).

Vegetation in built-up areas

The *vegetation built* zone is defined wherever the wake zone of any building intersects the footprint of a vegetation patch. Only the column of air located within the vegetation canopy belongs to the zone (cf Fig. 1c).

Vegetation in open areas

The *vegetation open* zone is defined wherever the footprint of a vegetation patch is not intersected by any building wake zone. The entire column of air (below, within and above the vegetation) belongs to the zone (cf Fig. 1c).

2.3.4 Wind factors calculation

Once the wind zone are defined, wind factors along the three components are set. They are defined as fraction of the wind speed at a given height and position and are Röckle zone dependent. The equations used to calculate these wind factors are described B. For a more visual representation of these equations, please refer to the wind field illustrated Fig. 1.

2.3.5 Management of zone interactions and superimpositions

The philosophy of the URock workflow to deal with zone interactions and superimpositions is mainly based on QUIC-URB method. For the reader willing to find the main physical motivations for the choice made in the URock method, please refer to Brown et al. (2009a, 2013). However, although the philosophy and main physical reason for their method are well described, it is difficult to discern a clear algorithm in the QUIC-URB method. This section tries to fill this gap.

Concerning zone interactions, the cavity zone of any stacked block may remove or create zones when some given conditions are met. In URock, it removes any rooftop zone and any downwind building zone respectively for the *cavity-rooftop* and *cavity-downwind facade* interactions (Fig. 12). Backward cavity and wake zones are also created in the case of the *cavity-upwind facade* interaction. They have the same size as forward cavity and wake zones except that they start from upwind facades instead of downwind facades and thus go in the opposite direction. Their wind factor for a same distance from wall and height is also identical as forward cavity and wake zones except that they are multiplied by a coefficient of attenuation. The value of this coefficient depends of the location of the upwind facade within the cavity zone. The value of the cavity zone wind factor at the top of the upwind facade is taken as attenuation coefficient. Backward zone creation removes all downwind zones (cavity, wake, and street canyon) which may be at this position. definition of the upwind stacked block: it starts from the upper part of the backward zones instead of the ground.

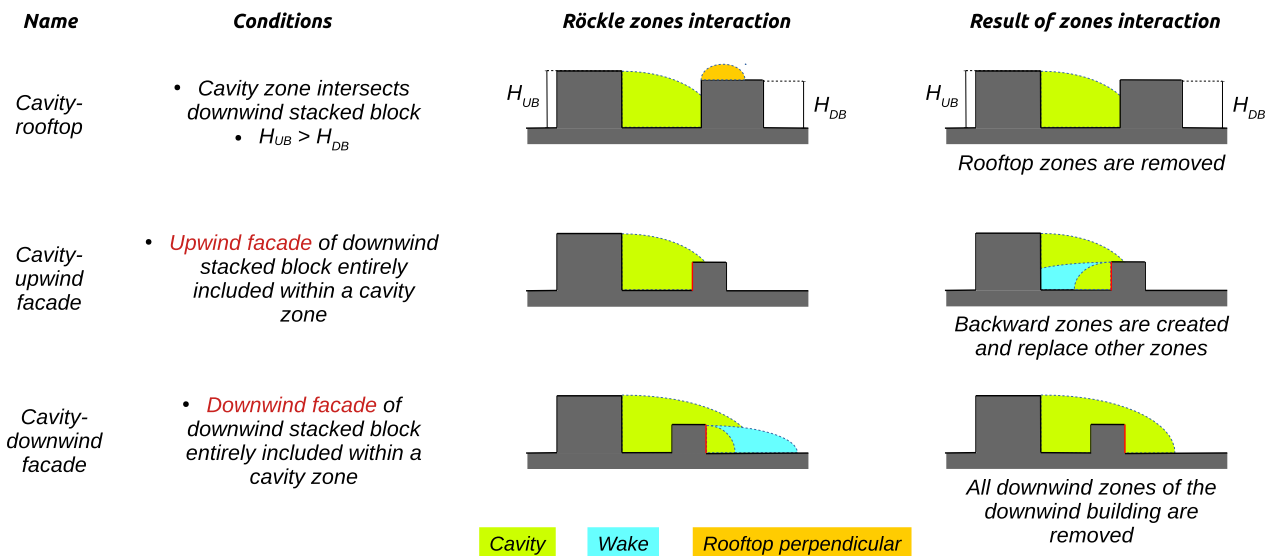


Figure 12. Description and results of the Röckle zone interactions implemented in URock.

Once these interactions are solved, some points of the space may be covered by several zones (Röckle zones superimposition). In this case, the following procedure is used (presented Fig. 13 and further described afterward):

1. Only forward building zones superimpositions are solved in order to have a single wind factor per point of the space,



- 245
2. Similar work is performed with backward building zones but previously weighted by forward wake zones,
 3. Forward and backward wind factors are merged (backward wind factors are used in case of zone intersections),
 4. The resulting wind factors are multiplied by vegetation weights when they intersect vegetation zones.

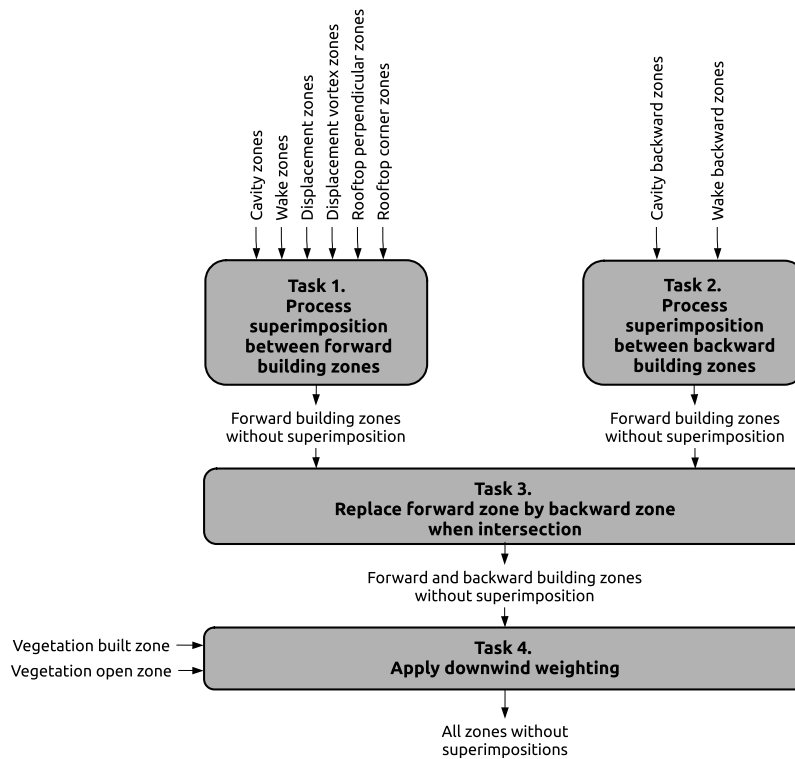


Figure 13. Workflow used to deal with zone superimposition

Step 1 consists in three tasks. The first task is to deal with superimposition happening between all building zones. To achieve this, the zone created by the most upstream stacked block is conserved (the origin of a zone is defined by the upwind facade for rooftop and displacement zones and by the downwind one for cavity, wake and street canyon zones). If equal, then the zone created by the upper stacked block is conserved. If equal, the conserved zone is defined using the following priority order: street canyon, cavity, rooftop perpendicular, rooftop corner, displacement vortex, displacement, wake. The second task is to deal with superimposition happening only between wake zones. The most upstream and highest stacked block rules described above is again used. The last task is to multiply the wind factors coming from task 1 by those obtained from task 2 only if those from task 2 come from a more upstream and highest stacked block.

Step 2 is quite similar to step 1. The first task is applied using backward cavity and backward wake zones but conserving zones created by the most downstream stacked block instead of the most upstream one. The second task is applied using only backward wake zone using the most downstream stacked block rule. The third task is also a combination of the results from



task 1 and task 2 but using the most downstream stacked block rule. A last task is added using the forward wake zone wind
 260 factors (obtained in step 1 task 2) to multiply the results from step 3.

Step 3 and 4 are simpler thus the description given previously is sufficient to understand what is performed. Fig. 14 illustrates the result of the whole superimposition procedure (considering only 5 zone types for the sake of simplicity: vegetation, cavity, wake, backward cavity and backward wake).

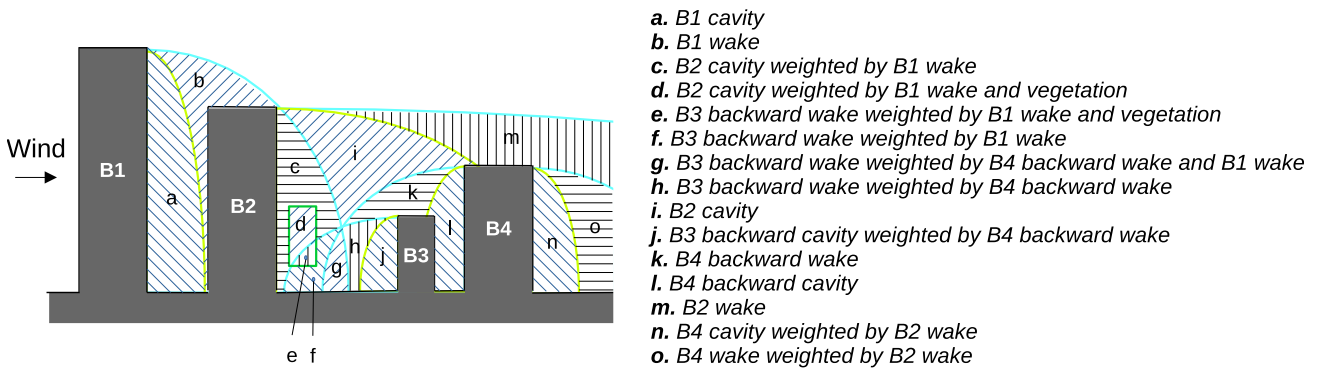


Figure 14. Example of zones resulting from the superimposition workflow

2.4 Wind speed calculation

265 The wind speed field calculation is performed in two steps: first the wind speed is initialized for all points of the domain and second the numeric wind solver is applied to balance the wind flow (Fig. 15).

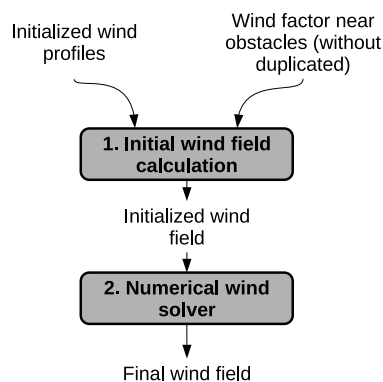


Figure 15. Procedure used to calculate wind speed field from vertical wind profile and wind factors

2.4.1 Initial wind field calculation

Once the wind factors WF are calculated and unique for any point of the space, they are used along with the vertical wind profile to initialize the wind speed field using Eq. 6.



$$270 \quad \begin{cases} U_0(x, y, z) = W_{F_U}(x, y, z) \cdot V_{wp}(x_{ref}, y_{ref}, z_{ref}) \\ V_0(x, y, z) = W_{F_V}(x, y, z) \cdot V_{wp}(x_{ref}, y_{ref}, z_{ref}) \\ W_0(x, y, z) = W_{F_W}(x, y, z) \cdot V_{wp}(x_{ref}, y_{ref}, z_{ref}) \end{cases} \quad (6)$$

where $U_0(x, y, z)$, $V_0(x, y, z)$, $W_0(x, y, z)$ the wind speed respectively along x , y and z axis for the point with coordinates x , y , z ; $W_{F_U}(x, y, z)$, $W_{F_V}(x, y, z)$, $W_{F_W}(x, y, z)$ the wind factor respectively along x , y and z axis for the point with coordinates x , y , z (default 1 is not covered by any Röckle zone); $V_{wp}(x_{ref}, y_{ref}, z_{ref})$ the along wind (y -axis) wind speed for the point at the reference position of the zone

275 Three definitions of $V_{wp}(x_{ref}, y_{ref}, z_{ref})$ exists depending on the zone:

1. the wind speed is taken at the top of the facade that corresponds to the beginning of the zone (note that in the current version of URock, the entire domain has the same vertical wind profile, thus only z_{ref} will affect $V_{wp}(x_{ref}, y_{ref}, z_{ref})$ value):

- (a) upwind facade for displacement, displacement vortex, backward cavity and backward wake zones,
- 280 (b) downwind facade for cavity and street canyon.

2. the wind speed at the location of the point of interest (x , y , z): wake, vegetation built and vegetation open zones (all weighting zones),

3. the wind speed at the reference height used in Eq. B5 and B6: rooftop perpendicular and rooftop corner zones.

2.4.2 Numerical wind solver

285 The last step of the methodology consists in balancing the air flow minimizing the modifications of the initialized wind field. To achieve this, the Lagrange multiplier λ in Eq. 7 is calculated. First, the initial wind field calculated at the center of each voxel is linearly interpolated to the voxel faces. Afterwards, an iterative process is used to calculate the 3D values of λ (for more detail concerning the numerical solver, please see Pardyjak and Brown (2003)).

$$E(u, v, w, \lambda) = \int_V [\alpha_1^2 \cdot (u - u_0)^2 + \alpha_1^2 \cdot (v - v_0)^2 + \alpha_2^2 \cdot (w - w_0)^2 + \lambda \cdot (\frac{\partial u}{\partial x} + \frac{\partial u}{\partial x} + \frac{\partial u}{\partial x})] \cdot dx \cdot dy \cdot dz \quad (7)$$

290 where $E(u, v, w, \lambda)$ the function to minimize, V the whole domain, α_1 and α_2 Gaussian precision moduli that can be used to favour modification of the wind field toward horizontal or vertical direction (by default set to 1), u , v , w the balance wind field, u_0 , v_0 , w_0 the initial wind field, dx , dy , dz the domain resolution along x , y and z axis



If $\lambda_{i,j,k}^t$ and $\lambda_{i,j,k}^{t+1}$ are λ values for cells located at coordinates i, j, k at iteration steps t and $t + 1$ respectively, we stop the iterative process when the condition described Eq. 8 is met.

$$295 \quad E = \sum_{i=1}^{nx} \sum_{j=1}^{ny} \sum_{k=1}^{nz} |\lambda_{i,j,k}^{t+1} - \lambda_{i,j,k}^t| < \epsilon \quad (8)$$

where ϵ the threshold value to stop iterations (default 0.0001)

Last, the wind velocity field is updated using the final λ values (Eq. 9). Note that the wind speed orthogonal to the boundary of a solid cell should be zero ($\frac{\partial \lambda}{\partial n}$) and at the inflow/outflow boundary, the initial wind profile should not be modified ($\lambda = 0$).

$$\left\{ \begin{aligned} u &= u_0 + \frac{1}{2 \cdot \alpha_1^2} \cdot \frac{\partial \lambda}{\partial x} v = v_0 + \frac{1}{2 \cdot \alpha_1^2} \cdot \frac{\partial \lambda}{\partial y} w = w_0 + \frac{1}{2 \cdot \alpha_2^2} \cdot \frac{\partial \lambda}{\partial z} \end{aligned} \right. \quad (9)$$

300 3 Model implementation

Currently, URock 2023a is openly available as a QGIS plugin in the Zenodo repository <https://zenodo.org/record/7681245> (the tool development is currently performed on GitHub at https://github.com/j3r3m1/urock_processing and will be soon continue at <https://github.com/UMEP-dev>). It is mainly coded in Python and can be used as a standalone python library. Most of the spatial analysis is performed using the H2GIS spatial database (Bocher et al., 2015). The wind solver is based on the Numba Python library to boost the calculations.

In QGIS, the following minimal informations are needed:

- geographical informations: one GIS layer for buildings or one for vegetation, with at least a single attribute for roof or crown top height from ground respectively,
- wind conditions: wind speed and direction at a given height or a wind direction and a file containing a wind profile (csv file with height as first column, wind speed as second column),
- cell size: the vertical and the horizontal resolution used for the wind solver,
- output height: one or several height for which the wind field is needed.

As output, URock 2023a can save the 3D wind field in a NetCDF file or wind information along one or several planes at a height defined by the user in two formats: a raster file containing the absolute wind speed or a vector file containing horizontal wind speed, vertical wind speed, absolute wind speed and wind direction.

Soon, URock 2023a will be integrated within the QGIS plugin called UMEP. Like any UMEP processor, URock comes with its own preprocessor called *urock_prepare* and its own postprocessor called *urock_analyser* (cf. workflow Fig. 16). The first is useful if the user has the building footprint (or vegetation) but without height attribute. If he has a Digital Surface Model (for building or vegetation) and a Digital Elevation Model, he can use *urock_prepare* to generate the building and vegetation file in the right format. The postprocessor is used once URock 2023a has been run and a NetCDF file saved to plot a section view of the wind along a line or a vertical wind profile averaging the wind within a polygon. These two modules are already



available on GitHub (at https://github.com/j3r3m1/urock_prepare and https://github.com/j3r3m1/urock_analyser respectively) but will be soon integrated within the UMEP project.

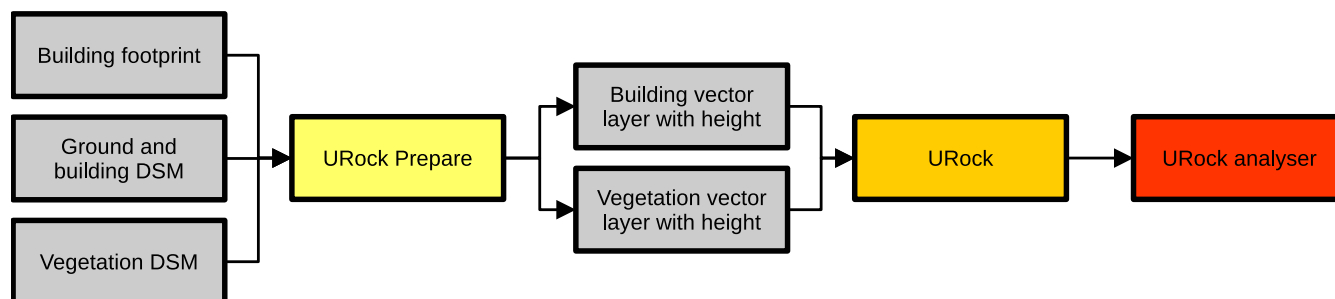


Figure 16. Workflow used to generate and analyse a wind field from raster data using URock and its related preprocessor and postprocessor

4 Model evaluation

325 In this section, URock (version 0.0.1) simulations are compared to QUIC-URB (version 6.4.1 in Matlab R2020b) simulations and wind tunnel measurements for both simple and more complex cases. Vertical and horizontal resolutions are set identically in URock and QUIC-URB. Preliminary investigations have shown a very limited effect of the resolution on the accuracy. Thus the main motivation for the resolution chosen in this paper is to facilitate the visual comparison between the models outputs and the measurements.

330 Spatial data and vertical wind profiles are set according to wind tunnel experiment parameters. All wind tunnel data are freely available on the AIJ website⁵.

4.1 Computation time

For each of the AIJ cases simulated using the URock model, the number of cells used for the calculation and the computation time are given Tab. 2. The calculations have been performed using a single processor (frequency of 2.3 GHz) of a personal
335 computer. The installed Random Access Memory of the computer is 16 GB. Note that the time presented also account for file loading (spatial information and wind conditions), initializing connection with the database used for spatial calculation and writing output files.

4.2 General agreement between URock and QUIC-URB

Based on the locations where the wind has been observed in the AIJ wind tunnel experiment, the correlation coefficient
340 calculated between URock and QUIC-URB is shown for horizontal, vertical or absolute wind speed for each of the test cases (Tab. 3).

⁵https://www.aij.or.jp/jpn/publish/cfdguide/index_e.htm (last access: 9 December 2022)



Table 2. Domain size used for the URock 2023a model to simulate AIJ cases and associated computation time

AIJ case	Number of cells	Calculation time (s)
AIJ_CaseA	199,778	23
AIJ_CaseB	314,415	23
AIJ_CaseC - from West	667,485	40
AIJ_CaseC - 22.5° clock-wise from West	786,236	33
AIJ_CaseE - 202.5° clock-wise from North	6,379,965	340
AIJ_CaseE - 90° clock-wise from North	5,967,360	318
AIJ_CaseG	280,112	33

Table 3. Correlation coefficients between URock and QUIC-URB for each AIJ cases

AIJ case	Horizontal	Vertical	Absolute
AIJ_CaseA - 1.25m	0.94	0.71	-
AIJ_CaseA - 12.5m	0.87	0.76	-
AIJ_CaseB - 1.25m	0.99	0.34	-
AIJ_CaseC – 0° from West	-	-	0.88
AIJ_CaseC – 22.5° clock-wise from West	-	-	0.88
AIJ_CaseE – 202.5° clock-wise from North	-	-	0.79
AIJ_CaseE – 90° clock-wise from North	-	-	0.82
AIJ_CaseG	-	-	0.42

QUIC-URB and URock show a good agreement for most of the cases. Two cases have particularly low correlation coefficient: case G and the vertical wind speed for case B. For the first case, the low score is only due to the fact that in this case, the spatial variations of the wind speed are very low (thus even a small difference leads to a considerable decrease of the correlation). For the latter case, the low score is mainly explained by only three points having really high value in QUIC while low in URock. However, these points are not relevant since they are associated to upward winds both in QUIC and URock while downward winds in the AIJ data (further discussed section 4.4).

In the next sections, QUIC-URB results are shown only when they differ sufficiently from URock results. Thus, most of the success and limitations that are shown for URock are also applicable for QUIC-URB.

350 4.3 Isolated building - square base

The building used for this case has a square base of size b and its height is twice its width ($h = 2 \cdot b$). More informations about the inflow wind profile and accurate sensor location can be found in the *case A* description on the AIJ website and also in MENG and HIBI (1998).



Horizontal wind vectors near the ground show a good agreement between models and observations. The main differences
 355 can be observed near the corner of the upwind facade where the cross-wind component is higher in the AIJ data than in URock.
 Absolute horizontal wind speed generally agree except in an along-wind ellipse located right beside the building edge (red
 ellipse Fig. 17a). Due to the absence of Rökke zone in this area, URock overestimates the wind speed (Fig. 17c).

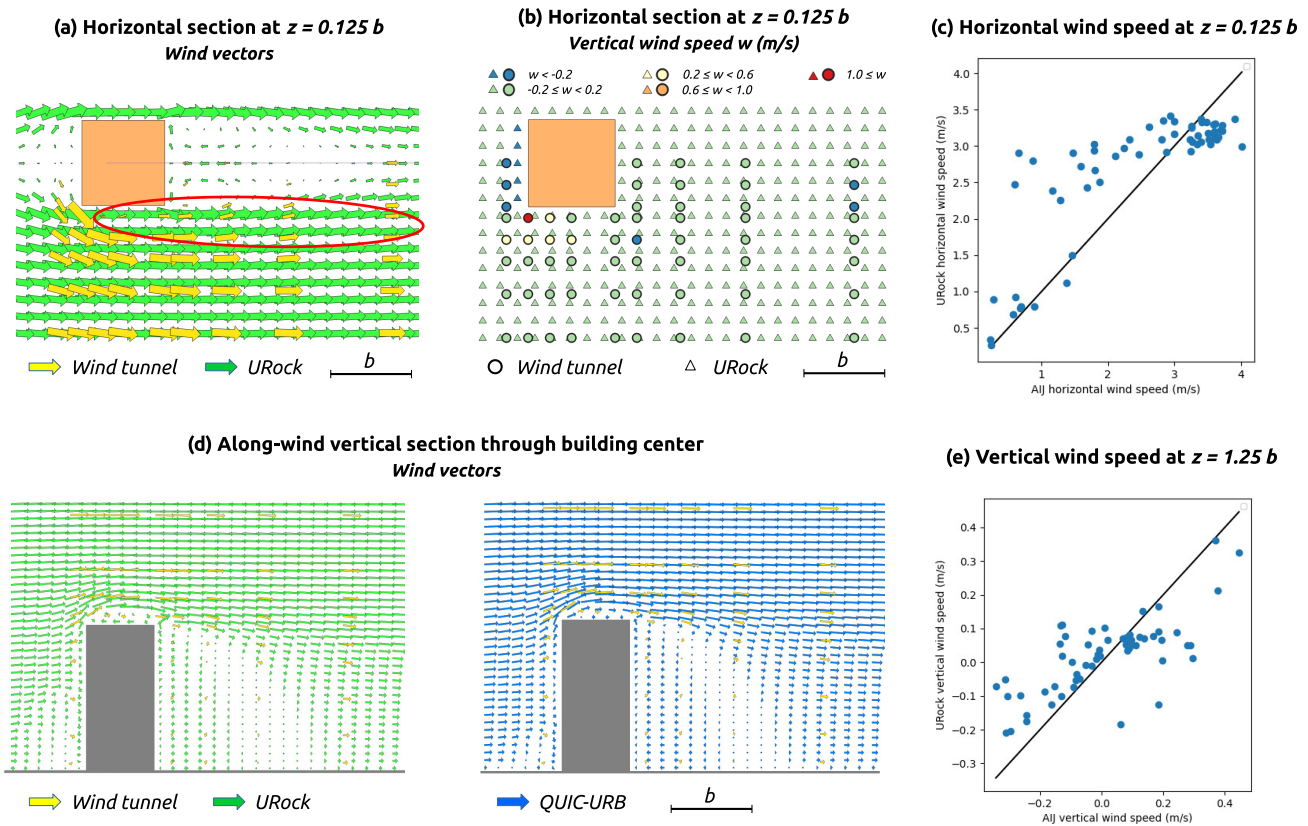


Figure 17. AIJ wind tunnel measurement as well as URock and QUIC-URB outputs for a square base isolated building

Near the ground ($z = 0.125 \cdot b$), URock vertical wind speed values are really low (included between -0.15 and 0.05 m/s)
 while observations show quite high wind speed locally (below 0.5 and above 1.5 m/s). The main spatial difference is located
 360 near the upwind edges of the building: the displacement vortex that goes cross-wind along the upwind facade is known to
 continue its way up and along-wind when it reaches the building corner. This leads to a non-negligible vertical component in
 this area as we can see Fig. 17b.

At higher level ($z = 1.25 \cdot b$), the absolute vertical wind values observed are lower (below 0.5 m/s) and URock captures well
 the spatial variability of the AIJ values (Fig. 17e).

365 Wind tunnel measurements have also been performed within an along-wind sectional plane located on the building center.
 The wind vectors in URock and QUIC-URB are quite consistent with those observed in the AIJ data. The main difference is



located at the top of the roof where a clear vortex structure is created in URock while it does not exist (or is limited in size) in the wind tunnel observation and in QUIC-URB (Fig. 17d).

4.4 Isolated building - rectangular base

370 The building used for this case has a rectangular base of width b (along-wind) and length equal to $4 \cdot b$ (cross-wind) while its height is also $4 \cdot b$. More informations about the inflow wind profile and accurate sensor location can be found in the *case B* description on the AIJ website.

URock model has the same qualities and shortcomings for the rectangular than for the square base case except that the following shortcomings are exacerbated. First, the cross-wind component of the AIJ vectors near the building corner is higher
375 than the along-wind one and this affects the wind direction of most of the wind vectors downstream (Fig. 18a). Second, the ellipse impacted by wind overestimation is slightly wider than previously.

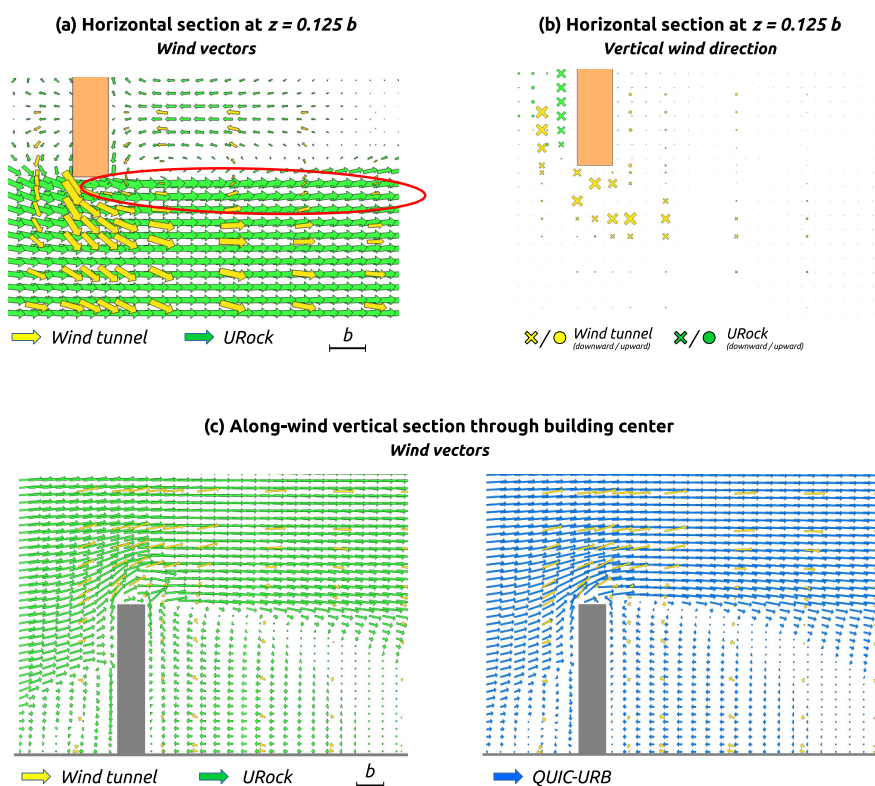


Figure 18. AIJ wind tunnel measurement as well as URock and QUIC-URB outputs for a rectangular base isolated building

One of the reasons for having low values for the cross-wind component near the building corner might come from an underestimation of downward wind in the displacement zone. In QUIC-URB and URock, a vortex is initialized in front of the upwind facade. This result in an downward wind close to the wall and an upward wind more upwind. According to Fig. 18b, it



380 seems either this zone is not relevant, either it has to be modified in order to have a downward wind where it currently has an upward wind.

The sectional plot shows a clear wind speed decrease of the AIJ measurement above the building cavity zone (in the rooftop zone and its prolongation - red ellipse Fig. 18c). This zone do not correspond to any Röckle zone and thus is overestimated by the URock model (and also the QUIC-URB one). In the square and rectangular building cases, the displacement zones
385 differ between URock and QUIC-URB: they are bigger in URock. While it does not impact much the wind field in the square building case (Fig. 17d), the differences are more pronounced in the rectangular case: the wind speed and direction near the ground is more consistent between URock and the AIJ data than in QUIC-URB and the AIJ data (Fig. 18c).

4.5 Regularly distributed cubes

The nine cubic buildings used for this case are regularly distributed in three rows of three buildings. The distance separating
390 each building is equal to the building width. More informations about the inflow wind profile and accurate sensor location can be found in the *case C* description on the AIJ website. Note that for this experiment, only the absolute wind speed is measured.

When the wind comes from the West, the scatterplot of URock versus AIJ wind speed looks quite similar as the one obtained for a single isolated building (Fig. 17c): half of the points follows well a (green) line parallel to the $y = x$ line and the other half is above this line (Fig. 19b). Most of the points located above the line belong to the red ellipses drawn Fig. 19a. A reduction
395 of the wind speed in these zones may then have a double positive impact: first the points have a good chance to get closer to the green dash line and second a reduction of the wind speed at the entrance of the streets may decrease the wind speed of all locations, thus decreasing the positive bias of the current URock version.

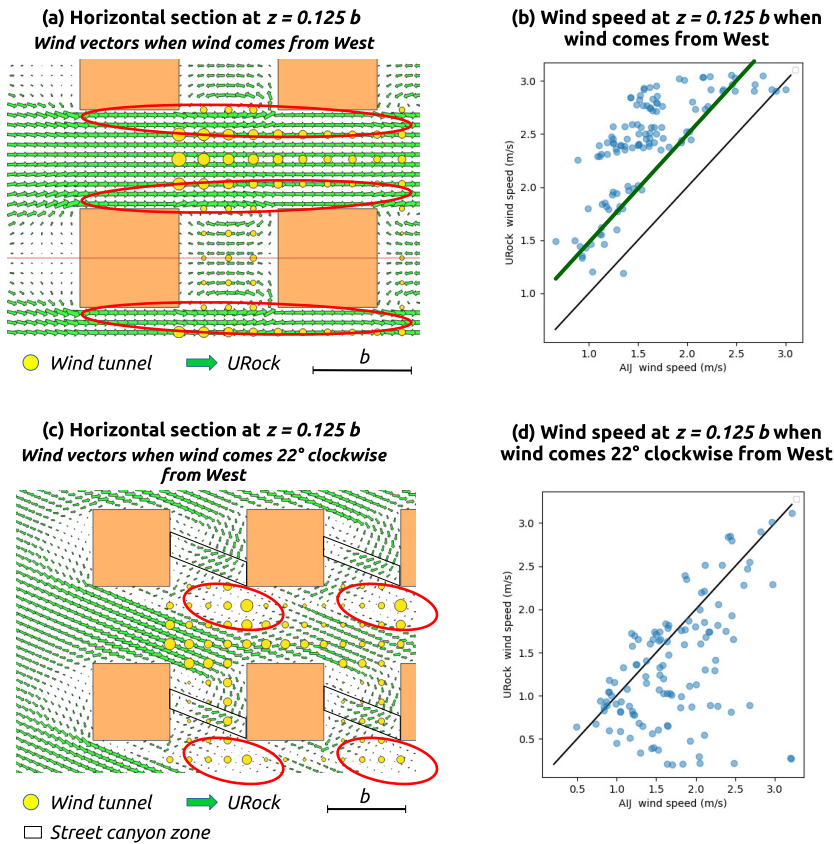


Figure 19. AIJ wind tunnel measurement and as URock outputs for regularly distributed cubes

When the wind comes 22.5° clockwise from the West, a large fraction of the location has a good agreement between URock output and observations (Fig. 19d). However, a non-negligible fraction of points are clearly underestimated by URock. The largest fail is located downwind most of the buildings, at the boundary between their cavity and wake zone (Fig. 19c). These underestimated zones are also downstream a small ray of street canyon zone. The conjunction of these zones induces a really small wind speed at the initialization stage (cavity/wake zone boundary) and no reason to get a much higher wind speed after the mass-balance stage since the wind in the street canyon zone is heading toward an other direction than the red ellipses.

4.6 Isolated tree

The tree used for this case has a 2 m width square base, its crown being located 1.2 m above ground level and extends up to 7 m. Its trunk is considered to have a negligible effect thus it is represented in URock. More informations about the inflow wind profile and accurate sensor location can be found in the *case G* description on the AIJ website.

In URock, a single isolated tree induces only a really small decrease of its downward wind speed. On the contrary, the AIJ wind tunnel data shows a considerable decrease: at 3 m high, the wind speed is reduced by about half of its initial value between



410 10 and 40 m downstream the tree (Fig. 20). The same level of magnitude is obtained by Li et al. (2023) when simulating (via
a CFD model) the wind around a tree canopy of 3.6 m wide, 3.6 m length and 5 m high. Recently, Margairaz et al. (2022)
updated the GES-Winds vegetation model for isolated trees: they have replaced the initial QUIC-URB vegetation model by
a new one having a wake zone downwind the tree. This model seems to show much better performance than the initial one.
Further wind tunnel or observations should be used to comfort this result but it seems that the vegetation zone model used in
415 URock and QUIC-URB needs to be updated.

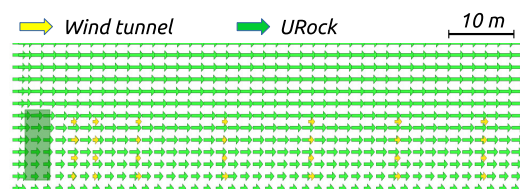


Figure 20. Wind vectors in an along-wind sectional plane located on the tree center: comparison between URock and AIJ wind tunnel measurement

4.7 Real urban setting

A real urban setting is used: it is a quite large city block with compact low-rise buildings. The wind tunnel observations are available for two cases: a potential future urban setting with three new high-rise buildings located on three existing large courtyards and the current urban setting with only the existing low-rise buildings. The first case has been chosen for URock
420 evaluation. More informations about the location and size of the buildings, the inflow wind profile and the accurate sensor location can be found in the *case E* description on the AIJ website or in Tominaga et al. (2005). Note that for this experiment, only the absolute wind speed is available.

When the wind comes from the East, the correlation between URock and AIJ windspeed is quite good, the scatterplot is quite close from the $y = x$ line although slightly below (Fig. 21b). However, about 10% of the locations are outliers: a major part
425 of them are overestimations (yellow triangles) and three points are underestimations (yellow diamond). Most of these points are located in the largest East North East street (Fig. 21a). Overestimation occurs on the northern part of the street while the underestimations are located at the intersection with the courtyard where is located the highest building (60 m high).

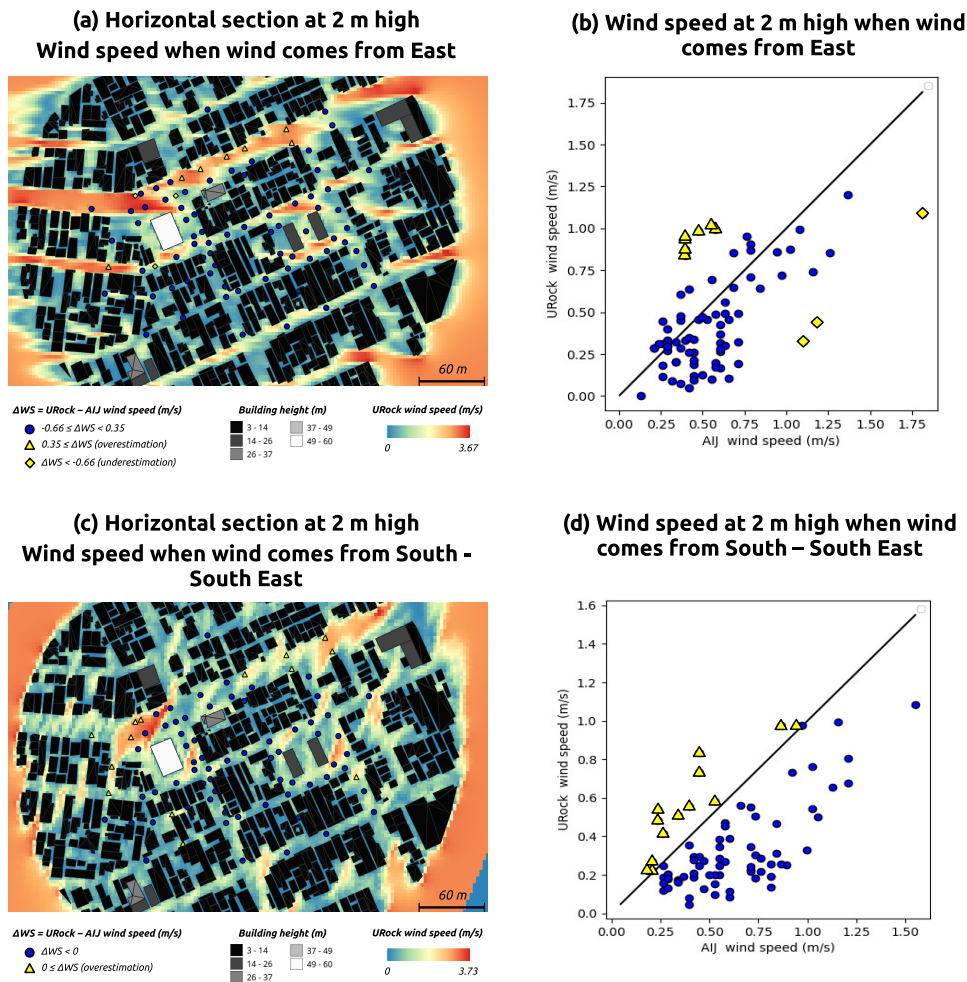


Figure 21. Comparison between URock outputs and AIJ wind tunnel measurement for a real urban setting at 2 m high

When the wind comes from the South South-West direction, the correlation between URock and AIJ windspeed is also quite good. There is a more pronounced underestimation of the wind speed which is quite similar for all AIJ wind speeds (Fig. 21d).
 430 Almost 20% of the locations are outliers (yellow triangles). All of them are overestimations and are most of them are located far from high-rise buildings (Fig. 21c). Most of them are also outside any building influence (quite far downwind any building), even though it is not the case for all locations. The central part of the zone equipped with wind sensors is not concerned by these outliers. Thus, the spatial variations in the zone of interest are quite well reproduced by URock, even though there is a general underestimation.



435 5 Conclusions

Most models dedicated to the calculation of wind speed in urban settings are intended to specialists, computationally intensive or implemented into proprietary softwares. The model presented in this manuscript (URock 2023a) will soon be available in the free and open source QGIS software within the UMEP plug-in. Its method is based on the so-called Röckle approach: first, the wind field near obstacles is initialized according to empirical rules drawn from wind tunnel observations; second, the air
440 flow is balanced minimizing the modification of the initial wind field. This method is reputed as quick but at our knowledge, only proprietary implementations exist. URock 2023a model is based on the Röckle zones implemented in the state of the art QUIC-URB software. The model method and implementation are described Sect. 2 and 3 respectively. Its evaluation is performed using both wind tunnel measurement (from the AIJ) and QUIC-URB outputs. This is a good opportunity to show that the results obtained with URock are (i) very close from the ones obtained with QUIC-URB, (ii) close from the ones
445 obtained in the wind tunnels for most cases, (iii) open to improvements in some cases (further described below).

In the isolated building cases (section 4.3, 4.4), the wind speed above the building and downstream do not perfectly fit the wind tunnel data. In the square base case, it seems the rooftop perpendicular zone is too much high while in the rectangular base case it seems the rooftop perpendicular zone should extend not only above the roof but also above the cavity zone (Fig. 18c). Currently, a rooftop zone stops when the roof ends even though the initial zone length is longer. A potential improvement
450 could be to keep the rooftop zone even though it is wider (along-wind) than the building width.

In the third case, when the wind comes from 22.5° clockwise from the left, some small street canyons are created. The wind direction in these zones might not be appropriate and be partially responsible for the nearby wind speed underestimations. In this configuration where the street canyon concept is not quite applicable (due to a very limited street canyon length), the wind flow should be modified in order not to have a brutal change of wind direction. Wind tunnel experiments where the effect of
455 length of the street canyon is investigated could be a good dataset for model improvements.

In the first three cases (section 4.3, 4.4 and 4.5), the agreement between the URock field and the wind tunnel data is quite good. Most of the differences observed might be attributed to the high wind speed values located in an along-wind ellipse starting from the upwind corner of the building. This zone is not defined as a Röckle zone while decreasing its wind speed at the initialization stage could solve most of the problems thanks to the mass-balance process:

- 460 – reduction of the final wind speed in this zone (Fig. 17),
- increase of the cross-wind component near the upwind corner (Fig. 17a),
- increase of the vertical component near the upwind corner (Fig. 17),
- decrease the global flow rate entering the streets and thus reducing the wind speed in most locations (Fig. 19a).

As a first attempt, a solution could also be only to delete the displacement vortex zone or set a downward wind in the displacement zone. Indeed, the analysis of the rectangular base case (B) showed that both URock and QUIC-URB have an upward
465 wind where AIJ data show downward. This modification may lead to modification in the upstream wind even though we do not expect it to solve all the problem.



The isolated tree case does not show a good agreement with the wind tunnel data (which are conformed by other literature results). It should be further verified using other wind tunnel or observation data and lead to modification of the vegetation
470 Röckle zones if needed.

There is a general wind speed underestimation when we compare URock with a compact urban setting. This result seems to have been identified in previous work (Girard et al., 2018). It seems that this behavior is exacerbated when the number of upstream buildings increases (direction SSW compared to E). While it seems that the spatial variations are quite well reproduced, investigations could be carried out to solve this limitation: the vertical wind profile could be updated to take into
475 account the morphometric characteristics of the urban setting.

Outside these model improvements, the model is currently limited to flat areas. A next version will account for complex terrain, taking into account the last literature updates on the field (Robinson et al., 2023).

Code and data availability. The comparison between model outputs (URock, QUIC-URB) and observation (AIJ wind-tunnel experiments) can be partially reproduced. The QUIC-URB model being a proprietary software, only its output wind fields can be shared. The corresponding
480 files are permanently available on Zenodo at <https://zenodo.org/record/7681245> along with the spatial data for each AIJ case (A, B, C, E and G), the URock 2023a software and all scripts needed for running the AIJ cases and comparing QUIC-URB, URock and AIJ wind fields. More information about the step by step procedure to reproduce the results can be found in the Readme file of the Zenodo repository.

Appendix A: Calculates building Röckle zones

This section contains more details about some of the building Röckle zones calculated in URock.

485 Displacement zone

The displacement zone is defined as a quarter of ellipse located on each upwind facade (cf Fig. 1a). The radius of the ellipse along the facade direction is half the facade length, the radius along the axis perpendicular to the facade (L_f) is defined by Eq. A1 and the vertical radius is 60% of the upwind facade height (H_F) (Kaplan and Dinar, 1996).

$$L_f = 1.5 \cdot \frac{W_{eff}}{1 + 0.8 \cdot \frac{W_{eff}}{H_F}} \quad (A1)$$

490 Displacement vortex zone

The displacement vortex zone is defined as a quarter of ellipse located on each upwind facade whenever the angle between the wind direction and an upwind facade $\theta_{wind/upwind_F}$ is within
[90-PERPENDICULAR_THRESHOLD_ANGLE, 90+PERPENDICULAR_THRESHOLD_ANGLE] (cf Fig. 1a). The size of the zone is identical in URock and QUIC-URB: the radius of the ellipse along the facade direction is half the facade length,
495 the radius along the axis perpendicular to the facade (L_{fv}) is defined by Eq. A2 and the vertical radius is 50% of the upwind facade height (H_F) (Bagal et al., 2004).



$$L_{fv} = 0.6 \cdot \frac{W_{eff}}{1 + 0.8 \cdot \frac{W_{eff}}{H_F}} \quad (A2)$$

Cavity zone

The cavity zone can be seen as a quarter of ellipse but having a slightly modified equation. If a standard ellipse has a fixed center, the one used in URock has a center which moves upon the along-wind direction, following the facade coordinates (cf. Fig. 1a). The Eq. A3 gives the modified ellipse coordinates for a wind parallel to the y-axis (in URock, all geometries are rotated in order to have wind coming along the y-axis - cf Sect. 2.1.2):

$$\frac{x^2}{W_{BBox}^2} + \frac{(y - y_{0_F}(x))^2}{L_r^2} + \frac{z^2}{H_F^2} = 1 \quad (A3)$$

where

x the coordinate of the ellipse along the x-axis

W_{BBox} the radius of the ellipse along x (corresponding to the cross-wind width of the stacked block)

y the coordinate of the ellipse along the y-axis

$y_{0_F}(x)$ the y-coordinate of the facade (may vary along the x-axis)

L_r the radius of the ellipse along y, defined by Eq. A4

z the coordinate of the ellipse along the z-axis

H_F the radius of the ellipse along z (corresponding to the facade height)

$$L_r = 1.8 \cdot \frac{W_{eff}}{\left(\frac{L_{eff}}{H}\right)^{0.3} \cdot (1 + 0.24 \cdot \frac{L_{eff}}{H})} \quad (A4)$$

Rooftop perpendicular zone

The rooftop perpendicular zone is defined as a half ellipse base cylinder cut along its height and located on each rooftop. It is only created when the angle between the wind direction and an upwind facade $\theta_{wind/upwind_F}$ is within [90-PERPENDICULAR_THRESHOLD_ANGLE, 90+PERPENDICULAR_THRESHOLD_ANGLE] (cf Fig. 1a). The cylinder height is the length of the upwind facade, the vertical diameter H_{cm} and the diameter perpendicular to the upwind facade d_{cp} are defined respectively by Eq. A5 and A6 (Pol et al., 2006).

$$H_{cm} = 0.22 \cdot (0.67 * MIN(H_F, W_{eff}) + 0.33 \cdot MAX(H_F, W_{eff})) \quad (A5)$$

$$\begin{cases} d_{cp} = L_{cp} \cdot \sin(\theta_{wind/upwind_F}) \\ L_{cp} = 0.9 \cdot (0.67 * MIN(H_F, W_{eff}) + 0.33 \cdot MAX(H_F, W_{eff})) \end{cases} \quad (A6)$$



Rooftop corner zone

The rooftop corner zone is defined as a square base oblique pyramid located on rooftop along an upwind facade with the apex starting from the most upwind point (cf Fig. 1a). The pyramid height is equal to the length of the upwind facade (L_{fc}) while the width of the pyramid base (L_{cc} is defined by Eq. A7 (Bagal et al., 2004).

$$525 \quad L_{cc} = 2 \cdot L_{fc} \cdot \tan(2.94 \cdot \exp(0.0297 \cdot (|\theta_{wind/upwind_F}| - \frac{\pi}{2}))) \quad (A7)$$

where $\theta_{wind/upwind_F}$ is the angle between the wind direction and an upwind facade (in radian)

Appendix B: Calculates wind factors

Wind factors along the three components are defined as fraction of the wind speed at a given height and position and are Röckle zone dependent. In this section, the Eq. used to calculate these wind factors are described. For a more visual representation of these equations, please refer to the wind field illustrated Fig. 1.

Displacement zone

In the displacement zone, the wind factors are defined according to Eq. B1 where $z < H_d$ Bagal et al. (2004).

$$\begin{cases} \frac{V_0(z)}{V_p(H_F)} = \frac{U_0(z)}{V_p(H_F)} = C_{dz} \cdot (\frac{z}{H_F})^p \\ H_d = 0.6 \cdot H_F \cdot \sqrt{(1 - \frac{D_y^2}{D_{od}^2})} \end{cases} \quad (B1)$$

where (cf Fig. B1)

535 D_y distance to wall along y axis

H_d ellipsoid height at the distance D_y

$C_{dz} = 0.4$

$p = 0.16$

z level of the cell

540 D_{od} length of ellipsoid along y axis at $z = 0$ m

θ angle between wind direction and perpendicular to the building wall

H_F building facade height

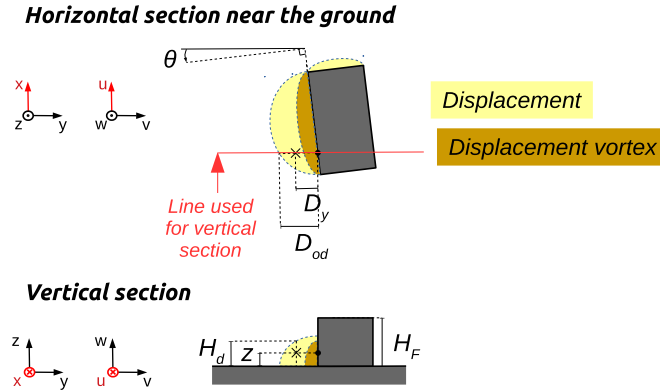


Figure B1. Variables needed for wind factor calculation in displacement zones

Displacement vortex zone

In the vortex zone, the wind factors are defined according to Eq. B2 where $z < H_{dv}$ (Bagal et al., 2004).

$$545 \quad \begin{cases} \frac{V_0(z)}{V_p(H_F)} = -[0.6 \cdot \cos(\frac{\pi \cdot z}{0.5 \cdot H_F}) + 0.05] \cdot 0.6 \cdot \sin(\frac{\pi \cdot D_y}{D_{odv}}) \\ \frac{W_0(z)}{V_p(H_F)} = -[0.1 \cdot \cos(\frac{\pi \cdot D_y}{D_{odv}}) + 0.05] \\ H_{dv} = 0.5 \cdot H_F \cdot \sqrt{1 - \frac{D_y^2}{D_{odv}^2}} \end{cases} \quad (B2)$$

where (cf Fig. B2)

D_y distance to wall along y axis

H_{dv} ellipsoid height at the distance D_y

$C_{dz} = 0.4$

550 $p = 0.16$

z level of the cell

D_{od} length of ellipsoid along y axis at $z = 0$ m

θ angle between wind direction and perpendicular to the building wall

H_F building facade height

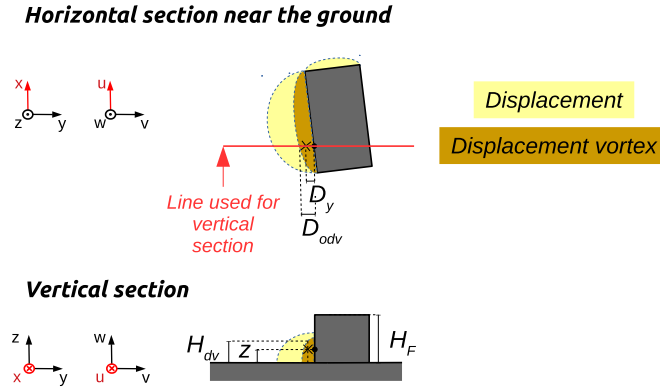


Figure B2. Variables needed for wind factor calculation in displacement vortex zones

555 **Cavity zone**

In the cavity zone, the wind factors are defined according to Eq. B3 where $z < H_c$ (Kaplan and Dinar, 1996).

$$\begin{cases} \frac{V_0(D_y, z)}{V_p(H)} = -\left(1 - \frac{D_y}{D_{oc} \sqrt{1 - \frac{z^2}{H^2}}}\right)^2 \\ H_c = H \cdot \sqrt{1 - \frac{D_y^2}{D_{oc}^2}} \end{cases} \quad (\text{B3})$$

where (cf Fig. B3)

D_y distance to wall along y axis

560 H_c ellipsoid height at the distance D_y

z level of the cell

D_{oc} length of ellipsoid along y axis at $z = 0$ m

H stacked block height

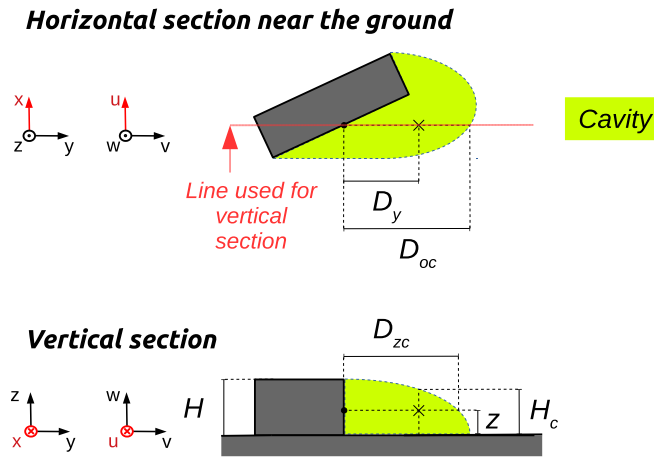


Figure B3. Variables needed for wind factor calculation in cavity zones

Wake zone

565 In the vortex zone, the wind factors are defined according to Eq. B4 where $z < H_w$ (Kaplan and Dinar, 1996).

$$\begin{cases} \frac{V_0(D_y, z)}{V_p(z)} = - \left[1 - \left(\frac{D_{oc}}{D_y} \right)^{1.5} \sqrt{1 - \frac{z^2}{H^2}} \right]^{1.5} \\ H_w = H \cdot \sqrt{1 - \frac{D_y^2}{D_{ow}^2}} \end{cases} \quad (\text{B4})$$

where (cf Fig. B4)

D_y distance to wall along y axis

H_w ellipsoid height at the distance D_y

570 z level of the cell

D_{ow} length of ellipsoid along y axis at $z = 0m$

H stacked block height

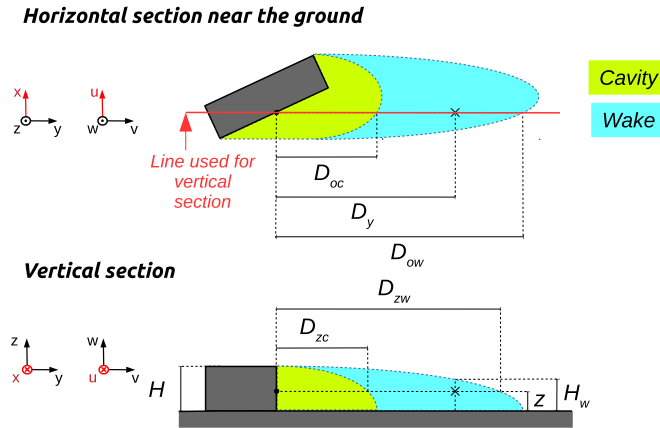


Figure B4. Variables needed for wind factor calculation in wake zones

Rooftop perpendicular zone

In the vortex zone, the wind factors are defined according to Eq. B5 where $H < z < H + H_r$ (Pol et al., 2006).

$$575 \quad \begin{cases} \frac{V_0(D_y, z)}{V_p(z_{ref})} = -\left(\frac{H+H_r-z}{z_{ref}}\right)^p \cdot \left|\frac{H+H_r-z}{H_r}\right| \\ H_r = H_{cm} \cdot \sqrt{1 - \left(\frac{D_y - \frac{L_{cp}}{2}}{L_{cp}}\right)^2} \end{cases} \quad (B5)$$

where (cf Fig. B5)

$p = 0.16$

$V(z_{ref})$ wind speed at measurement height z_{ref}

D_y distance to wall along y axis

580 H_r ellipsoid height at the distance D_y

H_{cm} maximum ellipsoid height

L_{cp} rooftop perpendicular length

z level of the cell

H facade height

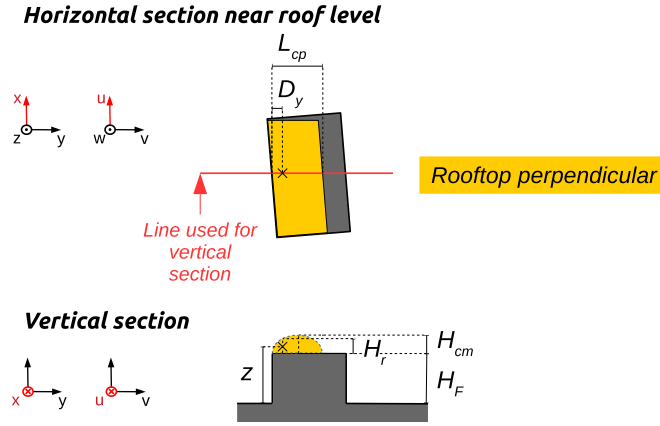


Figure B5. Variables needed for wind factor calculation in rooftop perpendicular zones

585 **Rooftop corner zone**

In the vortex zone, the wind factors are defined according to Eq. B6 where $H < z < H + H_{ccp}$ (Pol et al., 2006).

$$\begin{cases} \frac{U_0(D_y, z)}{V_p(z_{ref})} = -C1 \cdot \left(\frac{H+H_{ccp}-z}{z_{ref}}\right)^p \cdot \left|\frac{H+H_{ccp}-z}{H_{ccp}}\right| \cdot \sin(2 \cdot \Theta) \\ \frac{V_0(D_y, z)}{V_p(z_{ref})} = -C1 \cdot \left(\frac{H+H_{ccp}-z}{z_{ref}}\right)^p \cdot \left|\frac{H+H_{ccp}-z}{H_{ccp}}\right| \cdot \sin^2 \Theta \\ H_{ccp} = L_{ccp} = \frac{L_{cc} \cdot \sqrt{x_{Lp}^2 + y_{Lp}^2}}{L_{fc} \cdot \cos(\Theta - \widehat{SOP})} \\ C1 = \frac{1+0.05 \cdot W_{eff}}{H_F} \end{cases} \quad (B6)$$

where (cf Fig. B6)

$C1$ wind speed factor

590 H_F facade height

W_{eff} stacked block effective length

$V(z_{ref})$ wind speed at measurement height z_{ref}

H_r ellipsoid height at the distance D_y

H_{ccp} the H_{ccx} value for point p

595 L_{ccp} the L_{ccx} value for point p

L_{fc} the facade length

L_{cc} the L_{ccx} value at the end of the facade length

x_{Lcp} and y_{Lcp} absolute coordinates of vector L_{ccp}

z level of the cell

600 θ angle between wind direction and perpendicular to the building wall

\widehat{SOP} the angle between points S, O and P

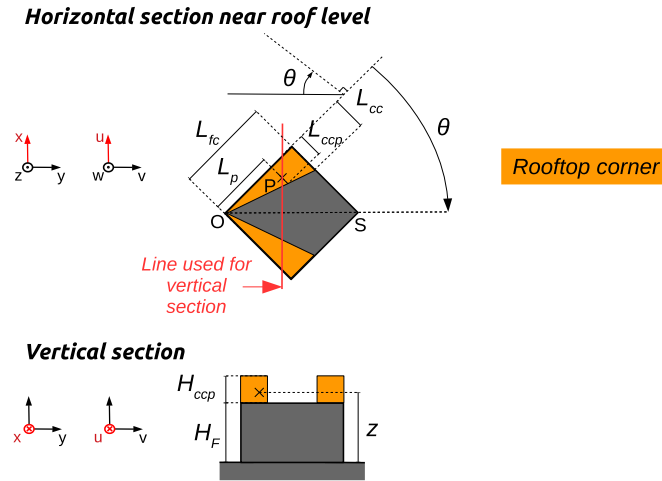


Figure B6. Variables needed for wind factor calculation in rooftop corner zones

Street canyon zone

In the street canyon zone, the wind factors are defined according to Eq. B7 where $H < z < H_{sc}$ and $z < H_c$ (adapted from Kaplan and Dinar (1996) and Singh et al. (2008)).

$$\begin{cases}
 \frac{U_0(D_y)}{V_p(H_{UB})} = \sin(2 \cdot \Theta) \cdot \left[0.5 + \frac{D_y \cdot (D_{os} - D_y)}{0.5 \cdot D_{os}^2} \right] \\
 \frac{V_0(D_y)}{V_p(H_{UB})} = \sin^2 \Theta - \cos^2 \Theta \cdot \frac{D_y \cdot (D_{os} - D_y)}{0.25 \cdot D_{os}^2} \\
 \frac{W_0(D_y)}{V_p(H_{UB})} = -\left| 0.5 \cdot \left(1 - \frac{D_y}{0.5 \cdot D_{os}} \right) \right| \cdot \left(1 - \frac{D_{os}}{0.5 \cdot D_{os}} \right)
 \end{cases} \quad (B7)$$

where (cf Fig. B7)

θ angle between wind direction and perpendicular to the downwind building wall

D_y distance along y axis from the upstream building wall

D_{os} distance between the upstream and the downwind buildings of the canyon

610 H_{UB} the upwind building height

H_{SC} the height of the lowest street canyon building

H_c ellipsoid height at the distance D_y (Eq. B3)

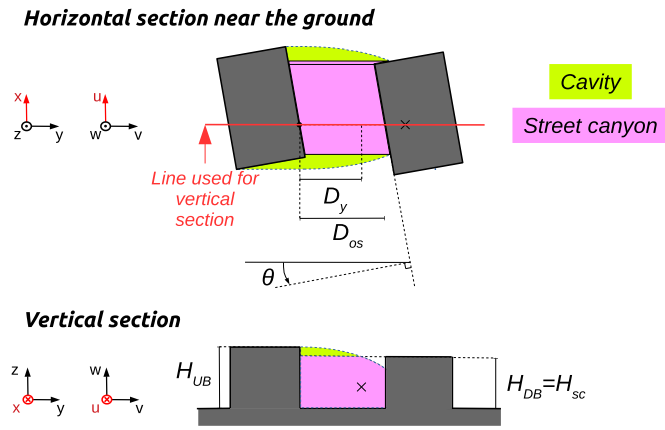


Figure B7. Variables needed for wind factor calculation in street canyon zones

Vegetation in built-up areas

In the *vegetation built* zone, the wind factors are defined according to Eq. B8 where $z < H_{vtm}$ (Nelson et al., 2009).

$$615 \quad \frac{V_0(z)}{V_p(z)} = \frac{\ln\left(\frac{H_{vtm}}{z_0}\right)}{\ln\left(\frac{z}{z_0}\right)} \cdot \exp\left(\alpha_i \cdot \left(\frac{z}{H_{vtm}} - 1\right)\right) \quad (B8)$$

where (cf Fig. B8)

H_{vtm} the maximum canopy height above the cell of interest

z_0 the roughness length of the surface

z level of the cell

620 α_i the attenuation factor of vegetation i ($=0$ if there is no vegetation at height z)

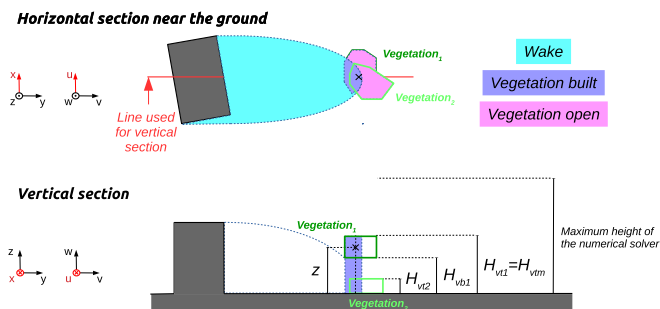


Figure B8. Variables needed for wind factor calculation in vegetation built zones

Vegetation in open areas



In the *vegetation open zone*, the wind factors are defined according to Eq. B9 where $z < H_{vtm}$ and to Eq. B10 where $z \geq H_{vtm}$ (Nelson et al., 2009).

$$\frac{V_0(z)}{V_p(z)} = \frac{\ln\left(\frac{H_{vtm}-d}{z_0}\right)}{\ln\left(\frac{z}{z_0}\right)} \cdot \exp\left(\alpha_i \cdot \left(\frac{z}{H_{vtm}} - 1\right)\right) \quad (\text{B9})$$

625

$$\frac{V_0(z)}{V_p(z)} = \frac{\ln\left(\frac{z-d}{z_0}\right)}{\ln\left(\frac{z}{z_0}\right)} \quad (\text{B10})$$

where (cf Fig. B9)

H_{vtm} the maximum canopy height above the cell of interest

d is the displacement length (Tab. 1)

630 z_0 the roughness length of the surface

z level of the cell

α_i the attenuation factor of vegetation i ($=0$ if there is no vegetation at height z)

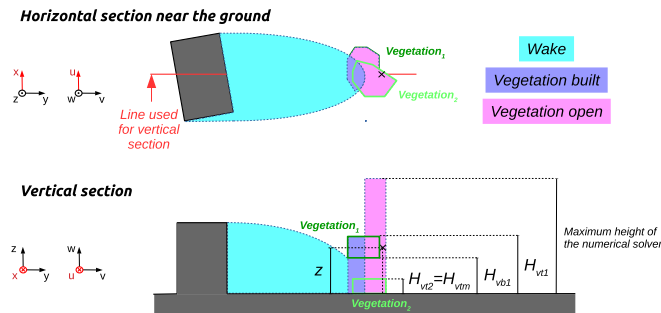


Figure B9. Variables needed for wind factor calculation in vegetation open zones

Author contributions. Conceptualization: JB, FL, SO / Data curation: JB / Formal analysis: JB, FL / Funding acquisition: JB, FL / Investigation: JB, FL / Methodology: JB, FL, SO / Project administration: JB / Resources: JB, FL, SO / Software: JB, FL, SO / Supervision: JB, FL
 635 / Validation: JB, FL, SO / Visualization: JB / Writing - original draft preparation: JB / Writing - review and editing: JB, FL, SO

Competing interests. The authors declare that they have no conflict of interest.

<https://doi.org/10.5194/egusphere-2023-354>

Preprint. Discussion started: 11 April 2023

© Author(s) 2023. CC BY 4.0 License.



Acknowledgements. This project has received funding from the European Union’s Horizon 2020 research and innovation programme under the Marie Skłodowska-Curie grant agreement No 896069.

We would like to thank the Architectural Institute of Japan for the data availability of their wind tunnel experiments. Thank you to
640 Yoshihide Tominaga for his answers concerning the datasets. We would also like to thank the Los Alamos laboratory to allow us freely using
the QUIC-URB software. Thank you to Michael Brown for his help and answers to our questions related to this model.



References

- Bagal, N., Pardyjak, E., and Brown, M.: Improved upwind cavity parameterization for a fast response urban wind model, in: 84th Annual AMS Meeting. Seattle, WA, 2004.
- 645 Bocher, E., Petit, G., Fortin, N., and Palominos, S.: H2GIS a spatial database to feed urban climate issues, in: 9th International Conference on Urban Climate (ICUC9), 2015.
- Bozorgmehr, B., Willemsen, P., Gibbs, J. A., Stoll, R., Kim, J.-J., and Pardyjak, E. R.: Utilizing dynamic parallelism in CUDA to accelerate a 3D red-black successive over relaxation wind-field solver, *Environ. Modell. Softw.*, 137, 104958, <https://doi.org/https://doi.org/10.1016/j.envsoft.2021.104958>, 2021.
- 650 Brown, M. J., Gowardhan, A., Nelson, M., Williams, M., and Pardyjak, E. R.: Evaluation of the QUIC wind and dispersion models using the Joint Urban 2003 field experiment dataset, in: AMS 8th Symp. Urban Env, 2009a.
- Brown, M. J., Gowardhan, A., and Pardyjak, E. R.: Evaluation of a fast-response pressure solver for a variety of building shapes and layouts, 2009b.
- Brown, M. J., Gowardhan, A. A., Nelson, M. A., Williams, M. D., and Pardyjak, E. R.: QUIC transport and dis-
655 persion modelling of two releases from the Joint Urban 2003 field experiment, *Int. J. Environ. Pollut.*, 52, 263–287, <https://doi.org/http://dx.doi.org/10.1504/IJEP.2013.058458>, 2013.
- Bruse, M.: ENVI-met 3.0: updated model overview, University of Bochum. Retrieved from: www.envi-met.com, 2004.
- Calzolari, G. and Liu, W.: Deep learning to replace, improve, or aid CFD analysis in built environment applications: A review, *Build. Environ.*, 206, 108315, <https://doi.org/http://dx.doi.org/10.1016/j.buildenv.2021.108315>, 2021.
- 660 Cionco, R. M.: A wind-profile index for canopy flow, *Bound.-Lay. Meteorol.*, 3, 255–263, <https://doi.org/http://dx.doi.org/10.1007/BF02033923>, 1972.
- Fröhlich, D.: Development of a microscale model for the thermal environment in complex areas, Ph.D. thesis, Dissertation, Albert-Ludwigs-Universität Freiburg, 2016, 2016.
- Fröhlich, D. and Matzarakis, A.: Spatial estimation of thermal indices in urban areas—basics of the SkyHelios model, *Atmosphere-Basel*, 9,
665 209, <https://doi.org/http://dx.doi.org/10.3390/atmos9060209>, 2018.
- Girard, P., Nadeau, D. F., Pardyjak, E. R., Overby, M., Willemsen, P., Stoll, R., Bailey, B. N., and Parlange, M. B.: Evaluation of the QUIC-URB wind solver and QESRadiant radiation-transfer model using a dense array of urban meteorological observations, *Urban climate*, 24, 657–674, <https://doi.org/http://dx.doi.org/10.1016/j.uclim.2017.08.006>, 2018.
- Hanna, S. and Britter, R.: Wind flow and vapor cloud dispersion at industrial sites. *Am. Inst. Chem. Eng-New York*,
670 <https://doi.org/http://dx.doi.org/10.1002/9780470935613>, 2002.
- Huttner, S. and Bruse, M.: Numerical modeling of the urban climate—a preview on ENVI-met 4.0, in: 7th international conference on urban climate ICUC-7, Yokohama, Japan, vol. 29, 2009.
- Johansson, L., Onomura, S., Lindberg, F., and Seaquist, J.: Towards the modelling of pedestrian wind speed using high-resolution digital surface models and statistical methods, *Theor. Appl. climatol.*, 124, 189–203, [https://doi.org/http://dx.doi.org/10.1007/s00704-015-1405-](https://doi.org/http://dx.doi.org/10.1007/s00704-015-1405-2)
675 2, 2016.
- Kaplan, H. and Dinar, N.: A Lagrangian dispersion model for calculating concentration distribution within a built-up domain, *Atmos. Environ.*, 30, 4197–4207, [https://doi.org/http://dx.doi.org/10.1016/1352-2310\(96\)00144-6](https://doi.org/http://dx.doi.org/10.1016/1352-2310(96)00144-6), 1996.



- Kastner, P. and Dogan, T.: Eddy3D: A toolkit for decoupled outdoor thermal comfort simulations in urban areas, *Build. Environ.*, 212, 108 639, <https://doi.org/http://dx.doi.org/10.1016/j.buildenv.2021.108639>, 2022.
- 680 Li, R., Zeng, F., Zhao, Y., Wu, Y., Niu, J., Wang, L. L., Gao, N., and Shi, X.: CFD simulations of the tree effect on the outdoor microclimate by coupling the canopy energy balance model, *Build. Environ.*, p. 109995, <https://doi.org/http://dx.doi.org/10.1016/j.buildenv.2023.109995>, 2023.
- Lindberg, F., Grimmond, C. S. B., Gabey, A., Huang, B., Kent, C. W., Sun, T., Theeuwes, N. E., Järvi, L., Ward, H. C., Capel-Timms, I., et al.: Urban Multi-scale Environmental Predictor (UMEP): An integrated tool for city-based climate services, *Environ. Modell. Softw.*, 685 99, 70–87, <https://doi.org/http://dx.doi.org/10.1016/j.envsoft.2017.09.020>, 2018.
- Macdonald, R.: Modelling the mean velocity profile in the urban canopy layer, *Bound.-Lay. Meteorol.*, 97, 25–45, <https://doi.org/http://dx.doi.org/10.1023/A:1002785830512>, 2000.
- Margairaz, F., Eshagh, H., Hayati, A. N., Pardyjak, E. R., and Stoll, R.: Development and evaluation of an isolated-tree flow model for neutral-stability conditions, *Urban Climate*, 42, 101 083, <https://doi.org/https://doi.org/10.1016/j.uclim.2022.101083>, 2022.
- 690 Maronga, B., Banzhaf, S., Burmeister, C., Esch, T., Forkel, R., Fröhlich, D., Fuka, V., Gehrke, K. F., Geletič, J., Giersch, S., et al.: Overview of the PALM model system 6.0, *Geosci. Model Dev.*, 13, 1335–1372, <https://doi.org/http://dx.doi.org/10.5194/gmd-13-1335-2020>, 2020.
- Matzarakis, A. and Endler, C.: Physiologically equivalent temperature and climate change in Freiburg, 2009.
- Matzarakis, A., Gangwisch, M., and Fröhlich, D.: RayMan and SkyHelios Model, in: *Urban Microclimate Modelling for Comfort and Energy Studies*, pp. 339–361, Springer, 2021.
- 695 MENG, Y. and HIBI, K.: Turbulent measurements of the flow field around a high-rise building, *Wind Engineers, JAWE*, 1998, 55–64, https://doi.org/http://dx.doi.org/10.5359/jawe.1998.76_55, 1998.
- Morille, B., Lauzet, N., and Musy, M.: SOLENE-microclimate: a tool to evaluate envelopes efficiency on energy consumption at district scale., *Energy Proced.*, 78, 1165–1170, <https://doi.org/http://dx.doi.org/10.1016/j.egypro.2015.11.088>, 2015.
- Musy, M., Azam, M.-H., Guernouti, S., Morille, B., and Rodler, A.: The SOLENE-Microclimat Model: Potentiality for Com-
700 fort and Energy Studies, in: *Urban Microclimate Modelling for Comfort and Energy Studies*, pp. 265–291, Springer, https://doi.org/http://dx.doi.org/10.1007/978-3-030-65421-4_13, 2021.
- Nelson, M., Addepalli, B., Hornsby, F., Gowardhan, A., Pardyjak, E., and Brown, M.: 5.2 Improvements to a Fast-Response Urban Wind Model, 2008.
- Nelson, M. A., Williams, M. D., Zajic, D., Brown, M. J., and Pardyjak, E. R.: Evaluation of an urban vegetative canopy scheme and impact
705 on plume dispersion, Tech. rep., Los Alamos National Lab.(LANL), Los Alamos, NM (United States), 2009.
- Pardyjak, E. R. and Brown, M.: QUIC-URB v. 1.1: Theory and User’s Guide, Los Alamos National Laboratory, Los Alamos, NM, 2003.
- Pol, S., Bagal, N., Singh, B., Brown, M., and Pardyjak, E.: Implementation of a rooftop recirculation parameterization into the quick fast response urban wind model, 2006.
- Ratto, C., Festa, R., Romeo, C., Frumento, O., and Galluzzi, M.: Mass-consistent models for wind fields over complex terrain: the state of
710 the art, *Environ. Softw.*, 9, 247–268, [https://doi.org/http://dx.doi.org/10.1016/0266-9838\(94\)90023-X](https://doi.org/http://dx.doi.org/10.1016/0266-9838(94)90023-X), 1994.
- Robinson, D., Brambilla, S., Brown, M. J., Conry, P., Quaife, B., and Linn, R. R.: QUIC-URB and QUIC-fire extension to complex terrain: Development of a terrain-following coordinate system, *Environ. Modell. Softw.*, 159, 105 579, <https://doi.org/http://dx.doi.org/10.1016/j.envsoft.2022.105579>, 2023.
- Röckle, R.: Bestimmung der Strömungsverhältnisse im Bereich komplexer Bebauungsstrukturen, Ph.D. thesis, 1990.
- 715 Sherman, C. A.: A mass-consistent model for wind fields over complex terrain, *J. Appl. Meteorol. Clim.*, 17, 312–319, 1978.



- Singh, B., Hansen, B. S., Brown, M. J., and Pardyjak, E. R.: Evaluation of the QUIC-URB fast response urban wind model for a cubical building array and wide building street canyon, *Environ. Fluid Mech.*, 8, 281–312, <https://doi.org/http://dx.doi.org/10.1007/s10652-008-9084-5>, 2008.
- 720 Tominaga, Y., Yoshie, R., Mochida, A., Kataoka, H., Harimoto, K., and Nozu, T.: Cross comparisons of CFD prediction for wind environment at pedestrian level around buildings, Part, 2, 2661–2670, 2005.
- Tominaga, Y., Mochida, A., Yoshie, R., Kataoka, H., Nozu, T., Yoshikawa, M., and Shirasawa, T.: AIJ guidelines for practical applications of CFD to pedestrian wind environment around buildings, *J. Wind Eng. Ind. Aerod.*, 96, 1749–1761, <https://doi.org/http://dx.doi.org/10.1016/j.jweia.2008.02.058>, 2008.
- 725 Wellens, A., Moussiopoulous, N., and Sahm, P.: Comparison of a diagnostic model and the MEMO prognostic model to calculate wind fields in Mexico City, *WIT Trans. Ecol. Envir.*, 3, 1970.